HUMAN-ROBOT INTERACTION

Human motor augmentation with an extra robotic arm without functional interference

Giulia Dominijanni[1], Daniel Leal Pinheiro[1,2]†, Leonardo Pollina[1]†, Bastien Orset[1], Martina Gini[3,4]‡, Eugenio Anselmino[3], Camilla Pierella[5], Jérémy Olivier[6], Solaiman Shokur[1,3]†, Silvestro Micera[1,3]†*

Extra robotic arms (XRAs) are gaining interest in neuroscience and robotics, offering potential tools for daily activities. However, this compelling opportunity poses new challenges for sensorimotor control strategies and human-machine interfaces (HMIs). A key unsolved challenge is allowing users to proficiently control XRAs without hindering their existing functions. To address this, we propose a pipeline to identify suitable HMIs given a defined task to accomplish with the XRA. Following such a scheme, we assessed a multimodal motor HMI based on gaze detection and diaphragmatic respiration in a purposely designed modular neurorobotic platform integrating virtual reality and a bilateral upper limb exoskeleton. Our results show that the proposed HMI does not interfere with speaking or visual exploration and that it can be used to control an extra virtual arm independently from the biological ones or in coordination with them. Participants showed significant improvements in performance with daily training and retention of learning, with no further improvements when artificial haptic feedback was provided. As a final proof of concept, naïve and experienced participants used a simplified version of the HMI to control a wearable XRA. Our analysis indicates how the presented HMI can be effectively used to control XRAs. The observation that experienced users achieved a success rate 22.2% higher than that of naïve users, combined with the result that naïve users showed average success rates of 74% when they first engaged with the system, endorses the viability of both the virtual reality–based testing and training and the proposed pipeline.

INTRODUCTION

Humans have always developed and used tools to increase their sensory and motor skills. Remarkable proficiency in tool usage is one of the main features of humankind and has had a fundamental role in our evolutionary process (*1*). A fascinating possibility is to increase our abilities even more by providing extra limbs to be worn and controlled by the users in addition to and simultaneously with the natural limbs. In the recent past, extra robotic limbs have moved from the purely fictional world to becoming exciting tools providing additional degrees of freedom for augmentation and restoration in able-bodied and clinical populations (*2*–*4*). Various prototypes characterized by different mechanical designs, actuation systems, and features have been proposed, with most robotic devices consisting of one or two arms or fingers. Extra robotic fingers have been tested in both augmentation and restoration applications, exploiting human-machine interfaces (HMIs) based on, among others, simple switch buttons (*5*), biological arm kinematics (*6*), toe-actuated force sensors (*7*), foot motion tracking (*8*), and muscle recordings (*9*–*11*).

Extra robotic arms (XRAs) instead focus primarily on augmentation. Their HMIs are often based on the use of foot movements (*12*–*18*)—a strategy that limits the walking possibilities of the users. Moreover, only a few have gone beyond their initial proof of concept, with limited functional characterization (*19*–*21*), and several examples limited their assessment to only virtual extra arms, without translation to a physical device (*12*, *15*–*17*). As we recently pointed out (*2*), neural resources allocation is a major challenge in the field. The identification and validation of sensorimotor control strategies that allow for independent and coordinated control with respect to the natural limbs represent the major concerns for the real-life use of XRAs, as well as the development of control strategies that do not hinder users' other capabilities. A few pioneering studies have started to systematically address this key issue, limiting their initial assessment to the control of two-dimensional (2D) or 3D cursors (*22*–*25*).

Here, we propose a comprehensive, step-by-step pipeline characterized by three different blocks (motor, sensory, and evaluation blocks) that methodically explores the identification of appropriate HMIs in the context of a designated task to be accomplished with XRAs. Following the motor and evaluation blocks of this pipeline, we assessed an intuitive and nonintrusive HMI that exploits two motor control modalities inherently independent from the biological limbs: gaze, which is naturally involved in reaching actions (*26*, *27*) and was previously used for target selection (*28*, *29*); and diaphragmatic respiration, which can be voluntarily modulated (*30*), is simple to monitor (*31*), and is coupled with voluntary actions (*32*–*35*) and self-awareness (*36*, *37*). Gaze was used to orient the trajectory (by selecting a target), whereas voluntary modulation of the diaphragm controlled the movement. The motor HMI operates within the task-extrinsic kinematic null space, encompassing motions of body parts not directly involved in the motor task (*2*). A sensory HMI consisting of a haptic feedback display was also developed to provide augmented tactile and proprioceptive information via skin vibration and indentation, by partially following the sensory block of the proposed pipeline. We chose to first integrate our HMIs for the control of an extra virtual arm (XVA) to validate their suitability. To this end, we developed a modular neurorobotic platform that integrates an

[1]Neuro-X Institute, Ecole Polytechnique Fédérale de Lausanne, Lausanne, Switzerland. [2]Neuroengineering and Neurocognition Laboratory, Escola Paulista de Medicina, Department of Neurology and Neurosurgery, Division of Neuroscience, Universidade Federal de São Paulo, São Paulo, Brazil. [3]BioRobotics Institute, Health Interdisciplinary Center, and Department of Excellence in AI and Robotics, Scuola Superiore Sant'Anna, Pisa, Italy. [4]Neuroelectronic Interfaces, Faculty of Electrical Engineering and IT, Rheinisch-Westfälische Technische Hochschule (RWTH) Aachen, Aachen 52074, Germany. [5]Department of Neurosciences, Rehabilitation, Ophthalmology, Genetics, and Maternal and Children's Sciences (DINOGMI), University of Genoa, Genoa, Italy. [6]Institute for Industrial Sciences and Technologies, Haute Ecole du Paysage, d'Ingénierie et d'Architecture (HEPIA), HES-SO University of Applied Sciences and Arts Western Switzerland, Geneva, Switzerland.
*Corresponding author. Email: silvestro.micera@epfl.ch
†These authors contributed equally to this work.
‡Present address: RWTH Aachen, Aachen, Germany.

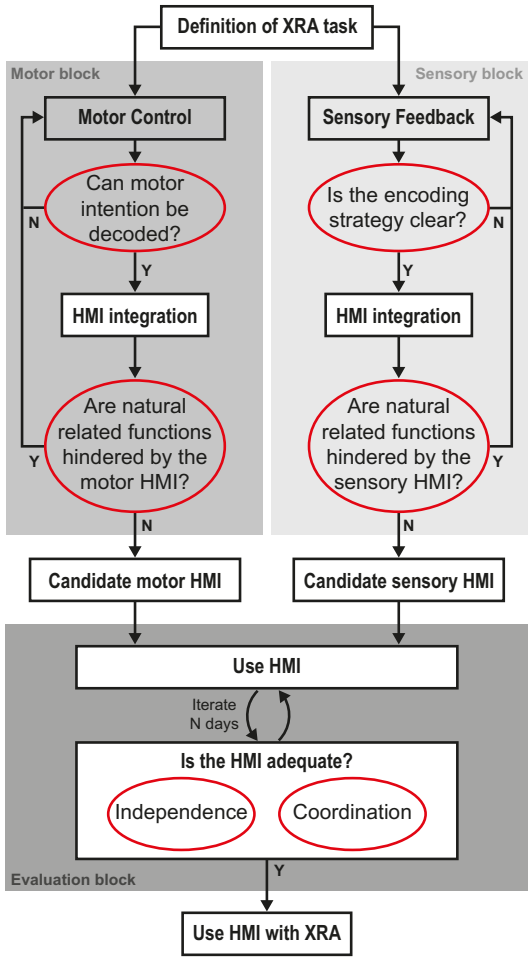

Fig. 1. HMI for XRA development pipeline. Proposed pipeline for the development of HMIs for XRAs given a defined task. The pipeline consists of three blocks: the motor block, the sensory block, and the evaluation block. Each block involves multiple stages.

immersive virtual environment (VE) and a bilateral upper limb exoskeleton allowing for powerful prototyping of immersive simulations (*38*) engaging the user and provided a flexible environment for testing different configurations, control strategies, and feedback approaches. Last, we assessed the ability of both experienced and naïve participants to control an XRA using a simplified version of our HMI.

To validate our approach, 65 healthy volunteers participated in a series of tests involving a variety of tasks, including some executed without visual input, to discern whether artificial haptic feedback affects performance. Here, we provide a detailed account of our proposed pipeline, the assessment of a multimodal HMI, and the insights gleaned from the application of our method. We believe that our findings contribute to the field and pave the way for more effective and efficient HMI design for XRAs.

RESULTS

A pipeline for the development of HMIs for XRAs

Here, we propose a general pipeline for developing motor, sensory, or sensorimotor HMIs for XRAs given a define task. The pipeline consists of three distinct blocks, one for the development of a candidate motor HMI (motor block), one for the development of a candidate sensory HMI (sensory block), and one comprising the evaluation steps for the considered HMI or their combination (evaluation block). The proposed components and steps of the blocks are depicted in Fig. 1 and detailed below.

Motor block

The first step consists of defining the motor control strategy, and it involves creating a strategy that outlines how the user will control the movement of the XRA with the motor HMI. This strategy should consider the motor intention, which is what the user aims to do with the XRA, and the possible ways to control the XRA, such as using direct brain-machine interfaces or indirect control through body movements or gestures.

Once a control strategy is in place, the second step consists of testing whether motor control intention can be decoded. The system should be tested to ensure that the HMI can successfully interpret and decode the user's intended movements. If this test fails, the control strategy needs to be reevaluated and adjusted.

In the third step, the HMI is integrated within the XRA. The system's software and hardware are made to work together, ensuring that commands from the HMI are correctly translated into movements in the XRA.

The fourth step consists of testing whether related natural functions are hindered. It is crucial that the HMI does not interfere with the user's natural movements or functionality. Given that it would be unfeasible and a waste of resources to test whether any of the biological functions the body can perform are impaired by the use of the HMI, this step involves first assessing which of the user's capabilities are likely to be hindered. In most cases, those would be the user's functions normally related to the biosignals used by the HMI (for example, the ability to balance and walk if the HMI is based on foot control). Once identified, testing can proceed to ensure that such functionalities are not impaired. Although the simultaneous testing of the task involving the control of the XRA and the task related to the biological functions investigated remains the main focus, a characterization of the latter alone might be deemed necessary in the case of a highly complex task. If the test fails, the process reverts back to step 1; otherwise, a candidate motor HMI that provides augmentation rather than resources rerouting has been found.

Sensory block

The first step consists of defining a sensory feedback approach. This step involves creating a plan for how the user will receive sensory feedback from the XRA via the sensory HMI. This feedback could include modalities such as pressure, temperature, or texture.

The second step entails testing whether the sensory encoding strategy is clear. The sensory feedback approach needs to be tested to ensure that the user can understand the sensory information delivered by the HMI. If this test fails, the sensory feedback approach needs to be reconsidered and adjusted.

Similar to the motor control section, the third step involves integrating the sensory HMI with the XRA to ensure that the information is correctly transmitted from the XRA to the user.

The fourth step encompasses testing whether natural functions are hindered. Just like in the motor block, the HMI should not interfere with the user's natural sensory flow at the HMI stimulation site. If this test fails, the process goes back to the first step; otherwise, a candidate sensory HMI has been found.

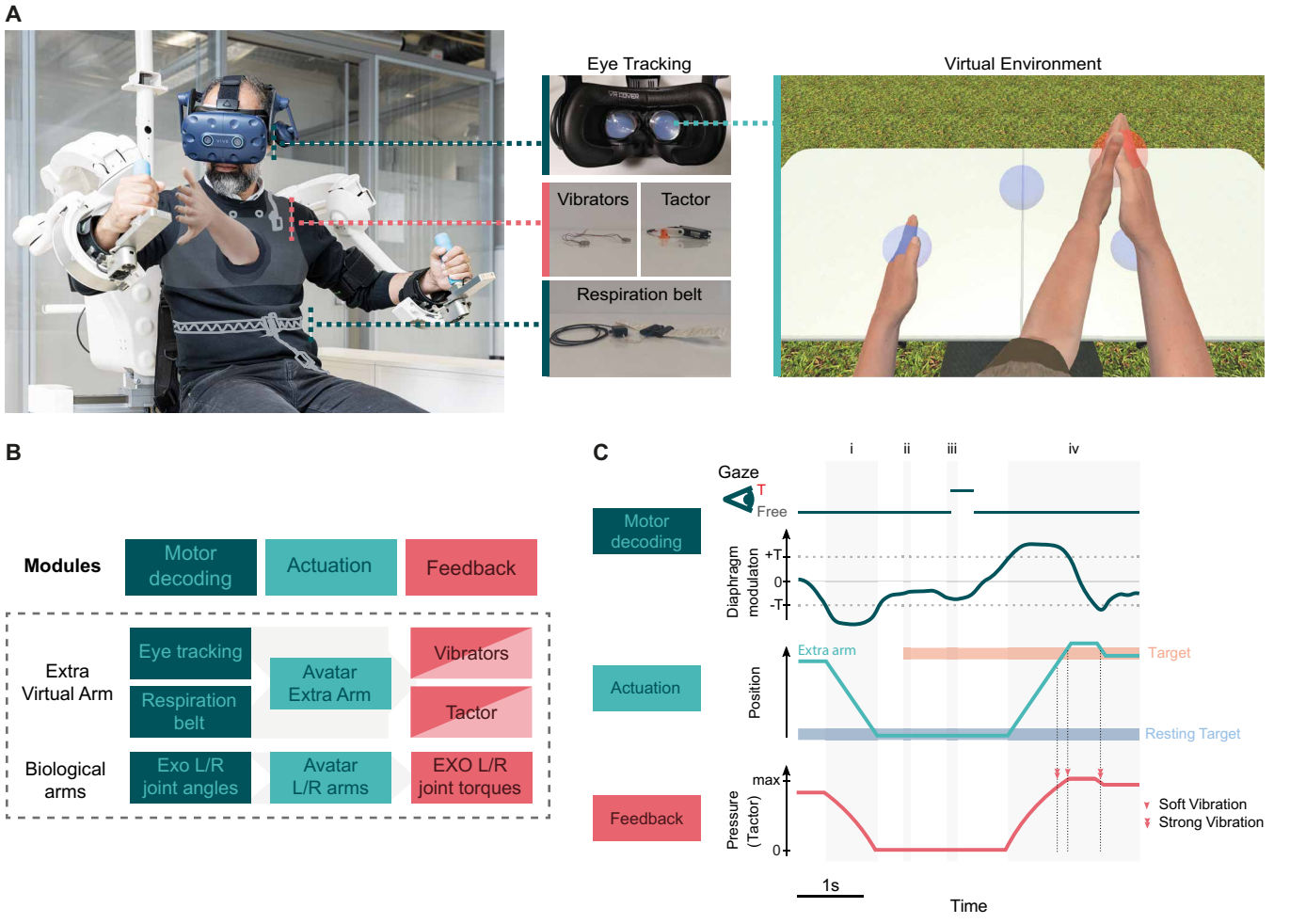

Fig. 2. Illustration of the neurorobotic platform and the HMI tested for extra arm control. (**A**) The neurorobotic platform setup and the motor and sensory HMI components. Image adapted with permission from M. Gafsou. The actuation of the XVA followed the motor decoding via eye tracking (Vive Pro Eye HMD; HTC Corporation, Taiwan) and via the decoding of diaphragm modulation with a respiration belt (Embla XactTrace, Natus). Artificial feedback was possible via a haptic display consisting of a tactor and vibrators. The actuation and force feedback of the avatar natural limbs occurred via the measurement of the joint angles and torques of the exoskeleton (ALEx, Wearable Robotics Srl, Italy). (**B**) Schematic of the various motor decoding, actuation, and feedback modules integrated in the neurorobotic platform. The lighter color in the feedback components indicate that they were not used for every user. (**C**) Example of motor decoding and actuation for a reaching movement with the XVA: (i) retracting the diaphragm below a given threshold brings the XVA to the resting target position; (ii) target appears; (iii) the user gazes at the target to select it; (iv) the user has to reach and maintain the position for 500 ms on the target. Feedback: The tactor encodes the distance of the XVA from the resting position. The pressure is null when the XVA is in the resting target. A strong vibration is given when the cursor enters the target (double arrow), and a soft vibration is given when it exits (single arrow) from the target.

Evaluation block

In this block, after the previous steps are successfully completed, the HMI is used with the XRA for a specific number of days (*N* days). This testing phase evaluates whether the HMI is adequate for the independent and coordinated use of the XRA with respect to the user's biological limbs. If the HMI passes this test, it is ready for use with the XRA.

Evaluation block definition is broad enough to encompass cases in which only a candidate motor or sensory HMI is tested as well as cases in which an integration of the two (a candidate sensorimotor HMI) is evaluated. In light of this, the outcomes from the evaluation block of different HMIs or combinations thereof can be compared to define an optimal HMI to use with the XRA. Moreover, the steps of the three blocks requiring the presence of the extra arm can be carried out in virtual reality.

Although the scope of the proposed pipeline is much broader than what can be thoroughly investigated in a single study, we believe that its comprehensive definition will help to frame and guide future works in the field. In this study, we primarily focused on the development of a candidate motor HMI following all the steps of the motor block and on its evaluation before use with an XRA. This was in itself a challenging undertaking that required the implementation of several subprojects related to motor control. However, we also designed a sensory HMI by only partially following the steps advised in the sensory block of the proposed pipeline, that is, without embarking on the complex assessment of the sensory complementary space (*2*) and potential hindrance of sensory functions. Such a choice was guided by the will to investigate whether the additional integration of a simple sensory HMI—although not ad hoc tested for human augmentation but rather leveraging the concept of sensory remapping and extensively used (in the present or

similar forms) for other applications (*5*, *39*, *40*)—would improve the outcome of the evaluation block compared with the sole use of the motor HMI.

The neurorobotic platform and the sensorimotor HMI

To apply the proposed pipeline for the development of an HMI for the control of reaching movements with an XRA, we developed a neurorobotic platform to enable testing and validation of the HMI in scenarios for human augmentation via extra arms (Fig. 2A). We used an immersive VE, where a humanoid avatar is endowed with an XVA anchored in a neutral position (the chest) and characterized by four digits and two thumbs to avoid association with a left or right hand. The VE's visual feedback, with the avatar rendered from a first-person perspective, was provided through the Vive Pro Eye head-mounted display (HMD, HTC Corporation, Taiwan). The VE is the core of our neurorobotic platform, which also integrates a bimanual upper limb exoskeleton [ALEx (*41*); Wearable Robotics Srl, Italy] used to track joint angles of and to provide force feedback to the biological upper limbs. Thanks to this platform and following different blocks of the proposed pipeline, it was possible to test with an XVA the suitability of a motor and a sensorimotor HMI—before use with an XRA—in an engaging simulation facilitated by the use of the bimanual exoskeleton, which ensured delivery of realistic force feedback to the biological arm about interactions in the VE.

For motor control, we developed an HMI that integrates the user's gaze and diaphragmatic respiration to control, respectively, the orientation and the movement of the extra arm. We used an eye-tracking system (integrated into the HMD) and a respiration belt (Embla XactTrace, Natus). The decoding approach was integrated in the system after proving adequate to decode the user's motor intention (see the Supplementary Materials and fig. S1).

We also developed an artificial haptic feedback module to provide tactile and proprioceptive information with vibration motors and a tactor. The system proved effective, with users able to link the received feedback with information about end-effector displacement (see the Supplementary Materials and figs. S2, S3, and S4), and the possibility of integrating this HMI component was therefore included in the neurorobotic platform. The different motor decoding, actuation, and feedback modules of the platform are depicted in Fig. 2B. Figure 2C shows an example of control with the proposed HMI for a single target-reaching action. To control the extra arm, users had to gaze at a given target appearing in the VE to select it and then could control the movement toward the target (or away from it) by expanding (or contracting) their diaphragm beyond a given threshold. To a subset of the users, haptic feedback was also provided; in this case, the tactor linearly encoded the distance from the resting state (the further the XVA, the stronger the pressure exerted by the tactor on the user's chest), and two coin vibrators encoded onset and offset contact with the target or the biological arms.

Our motor HMI did not affect visual exploration and speech

As a first step, we characterized our HMI (gaze and respiration) in the framework of human augmentation. We assessed whether it hindered two functions that could be affected by our HMI: the ability to visually explore the VE and the ability to speak. For this, we measured a baseline session with 10 naïve volunteers (5 females and 5 males, age = 25.7 ± 2.0) performing a unimanual reaching (UR) task with the XVA and compared it with a condition where they had to look for randomly appearing visual cues in their peripheral field of view in the VE during the UR task (UR-V). In a third block, they had to continuously count out loud while performing the same UR task (UR-C) (Fig. 3A). The UR-V and UR-C block order was counterbalanced. To ensure that the participants were not alternating between periods of XVA control and periods of counting, we measured the percentage of time where both tasks were performed simultaneously in the UR-C task. A low percentage here would mean that the participants segregated the two tasks. Our results showed that all participants managed to have moments of simultaneous control of the XVA and counting. The median score for all participants was above 47% (Fig. 3B).

We found no significant main effect of task type [$\chi^2(2) = 1.70$, $P = 0.428$, Bayes factor (BF) = 0.107], with volunteers performing similarly well in the UR task (63.33 ± 7.24%), the UR-V (58.5 ± 10.75%), and the UR-C (58.99 ± 6.66%) (Fig. 3C). Similarly, when looking at the error types associated with the different scenarios (Fig. 3D), we found comparable results for the three tasks. We divided the possible errors into three categories: no execution (NE, the XVA did not exit the rest position), timing error (TE, task time constraints not met), and wrong execution (WE, all other errors). Although we found an interaction between task and error types [$\chi^2(4) = 24.23$, $P < 0.001$], TE was the most frequent error for all three tasks {UR: 70.45, 95% confidence interval (CI) [61.36, 79.92]%, UR-V: 83.33, 95% CI [77.08, 90.96]%, UR-C: 66.67, 95% CI [56.52, 77.98]%} at $P < 0.0001$, with a significantly higher frequency in the UR-V compared with the UR-C task ($P = 0.0383$) and compared with the UR task (BF = 1.35). We also found that NE errors were more frequent ($P = 0.0492$) in the UR-C task (11.59, 95% CI [1.45, 22.91]%) than in the UR-V task (1.04, 95% CI [0.00, 8.67]%) and seemingly also in the UR task (1.13, 95% CI [0.00, 10.6]%, BF = 4.22). These last results are expected because, intuitively, VE is more likely to introduce a distraction, inducing TEs; in contrast, counting would more likely affect the ability to initiate movement control. We also found evidence that NE errors were more frequent than WE errors in the UR ($P = 0.0018$) and UR-C ($P = 0.0167$) tasks and limited evidence for the UR-V task (BF = 1.81). In the UR-V task, the majority of errors (~90%) were due to errors in the reaching task, with a smaller proportion (~9%) attributed to errors in both tasks, whereas only a single trial failure (~1%) was due to the VE task alone. Last, we investigated the mental workload by means of the NASA task load index (TLX) questionnaire for the three tasks. Once again, we found no evidence of a main effect of task [$\chi^2(2) = 4.05$, $P = 0.132$, BF = 1.03] for the cumulative score, with workload ratings of 54.80 ± 6.82 for the UR, 56.50 ± 7.82 for the UR-V, and 63.70 ± 8.30 for the UR-C tasks (Fig. 3E). In conclusion, our HMI protocol does not hinder the ability to visually explore and speak—a necessary condition for effective human augmentation.

Performance in independent XVA motor control improved with training

Twenty naïve volunteers (10 females and 10 males, age = 24.5 ± 4.4) were recruited for this study and randomly assigned to the motor-augmentation group. We assessed their motor control performance with the XVA (in terms of success rate and execution time) during various reaching tasks over three consecutive sessions. During each of the three sessions, participants completed blocks of UR in the VE (Fig. 4A) aimed at assessing their ability to control the XVA while maintaining the biological arms at rest. Participants improved their success rate over the three training sessions [$\chi^2(2) = 45.68$, $P < 0.001$], correctly succeeding in 75.8 ± 4.5% of the trials in the third session (Fig. 4B). Improvement took place prominently between the first and second sessions

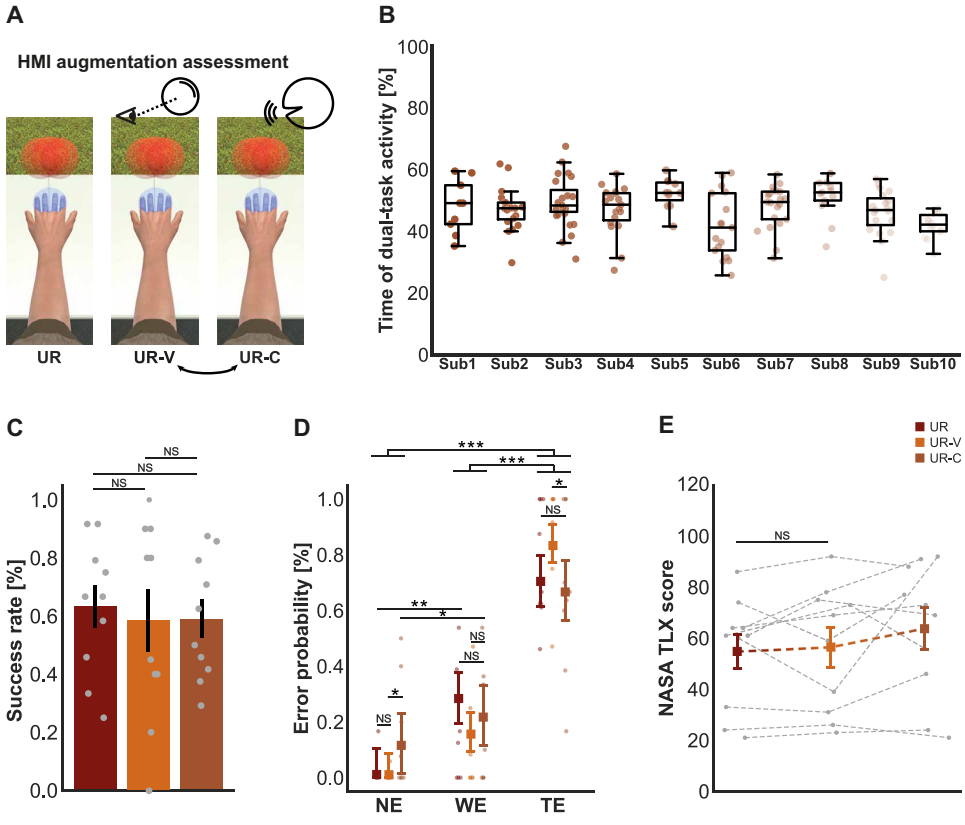

Fig. 3. HMI augmentation assessment. (**A**) Sketch representing the experimental design. The UR is shown together with the dual tasks involving UR and UR-V or UR-C. UR-V and UR-C were randomized in the order of performance to avoid a learning effect across tasks. (**B**) Relative amount of time spent speaking while also controlling the XVA. Values are reported for all participants. Each dot represents a trial being successful for the reaching task and not containing counting errors. (**C**) Average success rates across the 10 participants for the UR, UR-V, and UR-C. The error bars represent the SEM. Each point represents the success rate of a participant. For UR-V and UR-C only, those trials where both tasks were correctly executed were considered correct. (**D**) Error probability of NE errors, WE errors, and TEs for UR, UR-V, and UR-C. Error bars represent the multinomial CI. Each point represents a participant, with no point reported if the participant did not commit any error in the considered task. (**E**) Overall score of the NASA TLX questionnaire administered to the participants after each of the tasks. The marker represents the mean value across participants, whereas the bar stands for its SE. Asterisks indicate different levels of statistical significance: ***$P < 0.001$, **$P < 0.01$, and *$P < 0.05$. NS, nonsignificant difference (BF < 1).

(session 1: 56.7 ± 4.7%, session 2: 69.6 ± 4.9%, $P < 0.001$), but we found limited evidence for improvement between the second and third sessions (BF = 1.91). Volunteers also showed a similar trend for the execution times [main effect of session: $\chi^2(2) = 12.22$, $P = 0.002$], taking 4.0 ± 0.1 s to complete successful trials in the third session (fig. S5A). Execution time decreased from the first session to the second session (session 1: 4.3 ± 0.0 s, session 2: 4.1 ± 0.1 s, $P = 0.0445$) but not from the second session to the third session (BF = 0.139), indicating that participants reached a plateau.

Independent XVA motor control learning was retained

We invited 10 participants (5 females and 5 males, age = 25.4 ± 4.4) to come back for a fourth session 1 week after finishing their training. We found that learning was retained, with participants' success rate in the fourth session (81.7 ± 6.2%) higher but not significantly different [$\chi^2(1) = 1.45$, $P = 0.228$, BF = 0.44] than that attained in the third session by the motor-augmentation group (Fig. 4B). Similarly, as depicted in fig. S5, execution time in the fourth session (4.1 ± 0.1 s) was comparable with that reported for the motor-augmentation group in the third session [$\chi^2(1) = 2.03$, $P = 0.155$, BF = 0.23]. Preliminary results also showed how learning can be retained even 1 year after training (see the Supplementary Materials and fig. S6).

The primary error sources in independent XVA motor control were time constraint dependent

When investigating the sources of errors for the unsuccessful trials, we observed trends confirming what emerged when participants performed the UR task in the HMI augmentation assessment (Fig. 4C). Although an interaction between session and error type emerged [$\chi^2(6) = 45.18$, $P < 0.001$] and few within-error comparisons between sessions were found to be significant, no pattern emerged, and relevant comparisons (session 1 versus session 3 and session 3 versus session 4) showed no evidence of difference (BF < 0.3). We therefore restricted the subsequent analysis to the comparison of error types across sessions. As anticipated, we found that TE was the most frequent error ($P < 0.0001$), with an average frequency of 62.93, 95% CI [57.80, 67.8]%. Again, we also observed a higher average frequency of occurrence of WE errors compared with NE errors (WE: 26.71, 95% CI [22.29, 31.70]%; NE: 9.71, 95% CI [7.15, 13.0]%, $P < 0.001$).

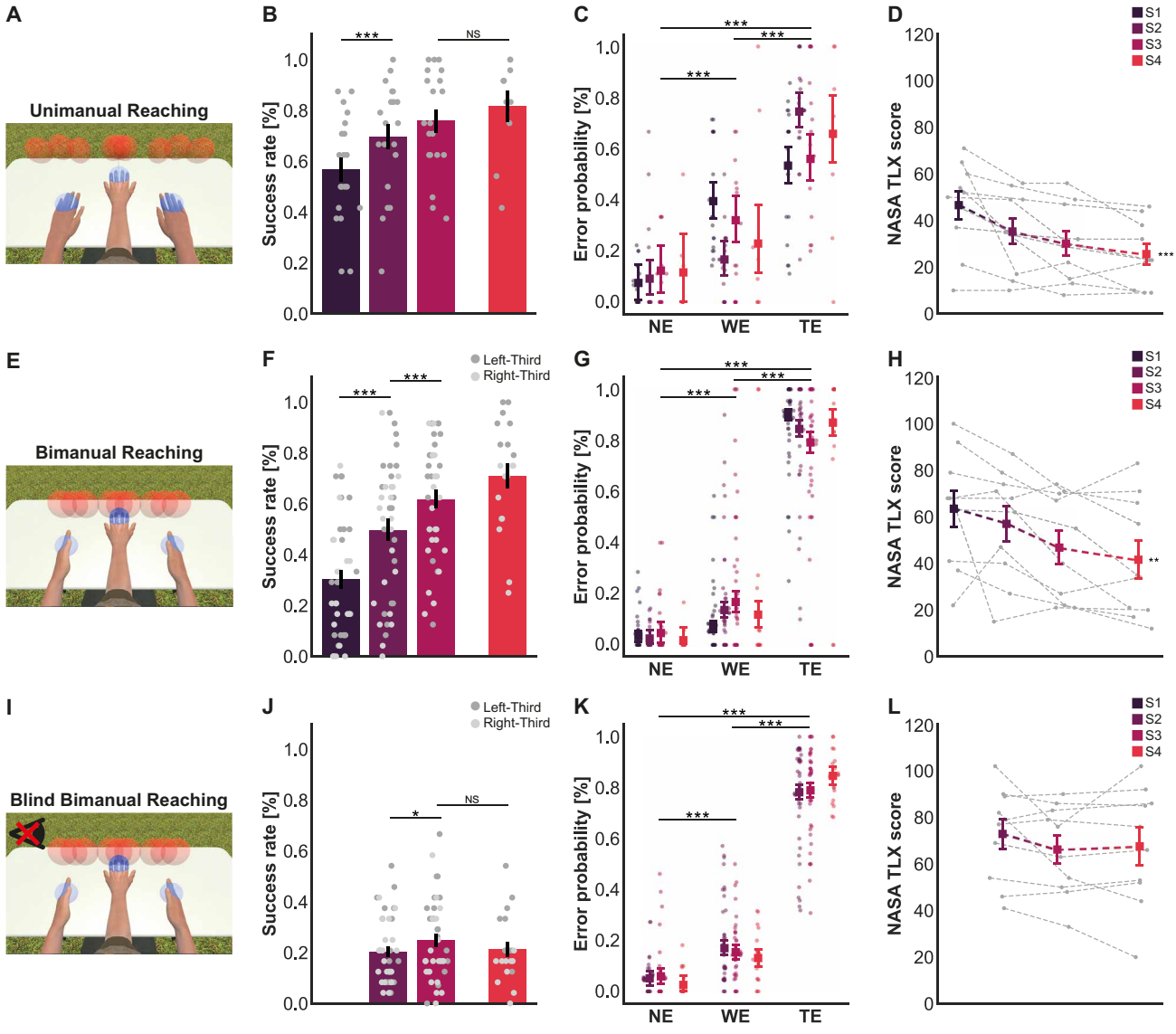

Fig. 4. Independent and coordinated motor XVA control. View of the VE for the XVA. (**A**) UR task, (**E**) BR task, and (**I**) B-BR task. Average success rates for the (**B**) UR task, (**F**) BR task, and (**J**) B-BR task performed with the XVA by the motor-augmentation group in the training sessions and in the fourth session. Error bars represent the SEM. Each point-color combination represents a participant. Error probability of NE errors, WE errors, and TEs for the (**C**) UR task, (**G**) BR task, and (**K**) B-BR task. Error bars represent the multinomial CI. Each point represents a participant, with no point reported if the participant did not commit any error in the considered session. Overall score of the NASA TLX questionnaire administered to the participants at the end of the (**D**) UR task, (**H**) BR task, and (**L**) B-BR task in each session. The marker represents the mean value across participants, whereas the bar stands for its SE; each point represents a participant. Asterisks indicate different levels of statistical significance: ***$P < 0.001$, **$P < 0.01$, and *$P < 0.05$. NS, nonsignificant difference (BF < 1).

Independent XVA motor control mental demand decreased with practice

We administered the NASA TLX questionnaire to the subset of 10 participants from the motor-augmentation group engaged in four sessions after each execution of the UR task. Participants reported decreased mental workload across sessions [$\chi^2(3) = 25.67$, $P < 0.001$], with a minimum of 28.6 ± 4.6 in the fourth session (Fig. 4D). With an inversed trend compared with the success rate, it emerged that participants not only improved in the UR task but also found it less demanding.

Performance in coordinated XVA motor control improved with training

In each of the three sessions, the motor-augmentation group participants were also asked to perform a bimanual reaching (BR) task in the VE to assess their ability to coordinate the XVA with one of their biological arms (Fig. 4E). Participants saw an increase in their success rate over the course of the three training sessions [$\chi^2(2) = 236.03$, $P < 0.001$]. By the third session, participants were accurately successful in $61.9 \pm 3.7\%$ of the trials, as depicted in Fig. 4F. They showed no sign of learning plateau,

with their performance improving between the first and second sessions (session 1: 30.4 ± 3.7%, session 2: 49.8 ± 4.3%, $P < 0.001$) as well as between the second and third sessions ($P < 0.001$). On the other hand, participants' BR task execution time was stable [$\chi^2(2) = 0.98$, $P = 0.614$, BF = 0.00033] across training sessions (session 1: 3.5 ± 0.1 s, session 2: 3.5 ± 0.1 s, session 3: 3.4 ± 0.1 s), suggesting that participants favored accuracy improvement over speed (fig. S5B).

Coordinated XVA motor control showed retention and continued improvement

Differently from the UR task and as depicted in Fig. 4F, participants engaged in the fourth session not only showed retention of learning for the BR task but their overall success rate (71.0 ± 4.8%) was also higher than that of the motor-augmentation group in session 3 [$\chi^2(1) = 15.11$, $P < 0.001$]. In contrast, execution time in the fourth session (3.2 ± 0.1 s) remained comparable with that shown by the motor-augmentation participants in the third session [$\chi^2(1) = 0.06$, $P = 0.807$, BF = 0.015], confirming the idea that accuracy was favored over speed in this task (fig. S5B).

The primary error sources in coordinated XVA motor control were time constraint dependent

Similar to the UR task, for the BR task (Fig. 4G), we found an interaction between session and error type [$\chi^2(6) = 52.62$, $P < 0.001$]. In this case, however, we saw a trend of change in error proportions across the three training sessions, with the frequency of WE errors increasing at the expense of that of TEs [session 1 versus session 2: $P = 0.026$ (WE), $P = 0.002$ (TE); session 2 versus session 3: $P = 0.58$ and BF = 0.20 (WE), $P = 0.20$ and BF = 0.41 (TE); session 1 versus session 3: $P < 0.001$ (WE and TE)]. Nonetheless, the situation stabilized in the fourth session—which, as we have seen, can be considered comparable with the training sessions—where proportions of WE errors and TEs attained an intermediate value between those of the first session and the third session, and no strong evidence of the difference between the frequency of these errors in the fourth session and in the three training sessions could be found ($P > 0.25$, BF < 0.65). NE errors instead remained stable and contained over the four sessions, with no evidence of a difference among the frequencies ($P > 0.3$ and BF < 0.54). Therefore, limiting the analysis to comparing error types across sessions, once again and even more evidently, we confirmed that overall TEs were also the most frequent in the BR task ($P < 0.001$), with an average frequency of 85.7, 95% CI [83.5, 87.6]%. WE error frequency was also higher than NE error frequency (WE: 11.6, 95% CI [9.8, 13.5]%; NE: 2.5, 95% CI [1.7, 3.7]%, $P < 0.001$). These results confirmed the same pattern of error proportions reported earlier.

Coordinated XVA motor control mental demand decreased with practice

After each execution of the BR task, we administered the NASA TLX questionnaire again to the subgroup taking part in four sessions. Once more, volunteers reported decreased mental workload across sessions [$\chi^2(3) = 15.57$, $P = 0.001$], with a minimum of 41.6 ± 8.1 in the fourth session (Fig. 4H). Therefore, volunteers not only demonstrated improvement in the BR task but also exhibited decreasing perception of its demand.

Coordinated XVA motor control in the absence of visual feedback improved with training

During days 2 and 3 of training, the motor-augmentation group participants were also asked to perform the BR task without visual rendering of the arms (blind) in the VE. The blind BR (B-BR) task was aimed at evaluating their XVA coordination ability without relying on visual feedback (Fig. 4I). As shown in Fig. 4J, participants improved their success rate from the second to the third session [session 2: 20.2 ± 2.1%, session 3: 24.9 ± 2.5%, $\chi^2(1) = 6.67$, $P = 0.01$]. Similar to what was found for the BR task, execution time for the B-BR task remained consistent [$\chi^2(1) = 1.19$, $P = 0.276$, BF = 0.192] in the two training sessions (fig. S5C).

Coordinated blindfolded XVA motor control showed retention

Participants engaged in the fourth session also showed retention of learning for the B-BR task [$\chi^2(1) = 1.82$, $P = 0.178$, BF = 0.378], although their overall success rate (21.2 ± 2.9%) seemed lower than the one of the motor-augmentation group in the third session (Fig. 4J). Again, in line with what was found for the BR task, execution time in the fourth session for the B-BR task (3.4 ± 0.1 s) remained comparable with what was shown by the motor-augmentation participants in the third session [$\chi^2(1) = 1.06$, $P = 0.302$, BF = 0.182], as shown in fig. S5C.

The primary error sources in coordinated blindfolded XVA motor control were time constraint dependent

Once again, for the B-BR task (Fig. 4K), we found an interaction between session and error type [$\chi^2(4) = 17.66$, $P = 0.001$]. In this case, we saw a change in error proportions in the fourth session compared with the second and/or third sessions for the NE errors in favor of TEs (BF > 1.3). However, we considered the actual effect size negligible compared with the differences between proportions across sections and therefore proceeded as in the previous cases to focus on the overall difference in error proportions. Again, TE was the most prominent error source, with a frequency of 80.8, 95% CI [78.8, 82.6]% ($P < 0.001$), followed by WE error, whose frequency was higher than NE error frequency (WE: 15.0, 95% CI [13.3, 16.8]%; NE: 4.1, 95% CI [3.2, 5.3]%, $P < 0.001$).

Stable coordinated blindfolded XVA motor control mental demand

As with the UR and BR tasks, after each execution of the B-BR task, we administered the NASA TLX questionnaire to the subgroup of participants taking part in the training (in the second and third session) and in the fourth session. In this case, we did not find evidence for changes in task workload over sessions [$\chi^2(2) = 3.53$, $P = 0.171$, BF = 1.01]. As shown in Fig. 4L, the minimum score was reported for the third session (66.2 ± 6.1). Therefore, although volunteers demonstrated improvement in the B-BR task, they showed a consistent perception of its demand.

Motor training resulted in agency but not ownership over the XVA

We assessed the subjective sense of embodiment of the XVA using a questionnaire adapted from (*7*). Participants rated their agreement with statements that were proxies for different embodiment features (agency, ownership, somatosensation, and body image). Volunteers

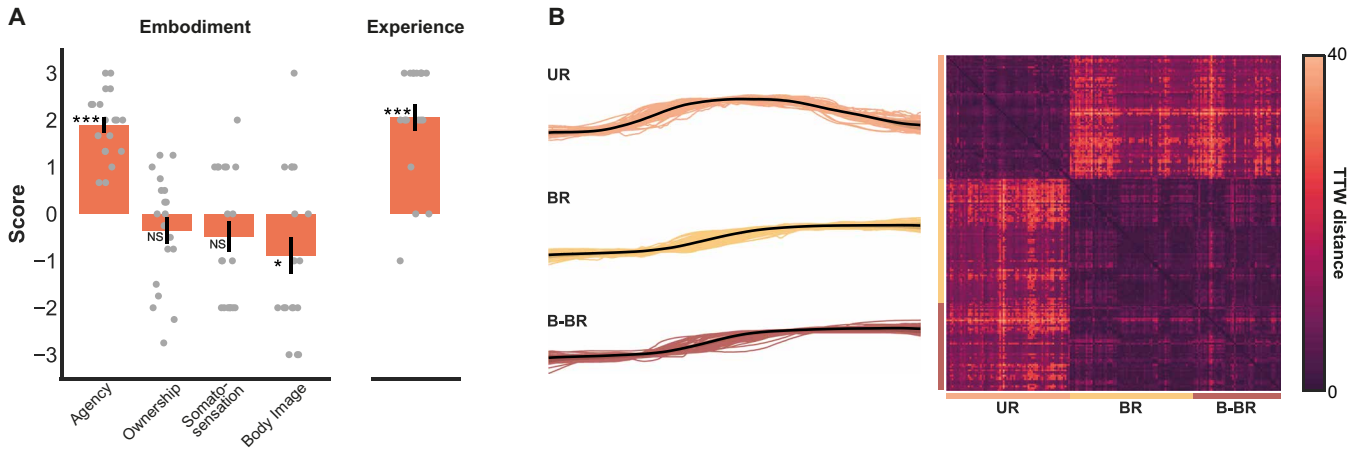

Fig. 5. XVA embodiment and respiration analysis for the motor-augmentation group. (**A**) Results of the questionnaire aiming to evaluate the embodiment and the experience with the XVA for the motor-augmentation group. The average scores are plotted for the different questions of the questionnaire together with the SEM. Each dot represents the score for a participant. (**B**) Average session participant respiration profiles in the UR, BR, and B-BR tasks and distance matrix.

were also asked to express whether they enjoyed the experience. Additional control questions were included in the questionnaire to assess their reliability in answering the questionnaire. One participant from the motor-augmentation group was excluded from the analysis because their control question average score exceeded 0 (neutral). As reported in Fig. 5A, the motor-augmentation participants reported agency over the XVA (score: 1.89 ± 0.16, $t_{18} = 11.60$, $P < 0.0001$) and neutral feelings relative to ownership of the XVA (score: -0.35 ± 0.28, $t_{18} = -1.28$, $P = 0.216$, BF = 0.483) and somatosensation (score: -0.47 ± 0.33, $Z = -1.61$, $P = 0.113$, BF = 0.822). They instead were in slight disagreement on incorporation of the XVA in their body image (score: -0.89 ± 0.39, $t_{18} = -2.30$, $P = 0.034$). Finally, volunteers rated the experience positively (score: 2.05 ± 0.28, $Z = 3.36$, $P < 0.001$).

Task-dependent diaphragmatic respiration profiles for XVA motor control

We analyzed the diaphragmatic respiration profiles of successful trials to understand the underlying control strategy participants used in UR and BR task types. We found that profiles from UR and from BR and B-BR successful trials were inherently different and could be divided into two separate clusters (Fig. 5B and fig. S7). UR profiles had a characteristic bell shape, which reflects the requirement of reaching the target and stopping inside it. BR and B-BR profiles instead were characterized by a sigmoid shape. This shows how participants were successfully accomplishing the BR and B-BR when collision of the XVA with the biological hand inside the target happened while the XVA was in motion. As evident from the matrices in Fig. 5B, respiration profiles exhibited unexpectedly small variations within tasks. The dendrogram in fig. S7 shows that increasing the number of clusters from two to three did not produce a separation for BR and B-BR, but, rather, four observations of the UR were included in the third cluster, which reveals that the BR and B-BR tasks were not different in terms of diaphragmatic respiration profiles.

Integration of artificial haptic feedback did not improve independent XVA control

To assess whether the integration of haptic feedback providing information on the XVA could boost performance, we recruited 10 naïve volunteers (5 females and 5 males, age = 22.2 ± 2.4) and assigned them to the sensorimotor-augmentation group. Mirroring what was done with the motor-augmentation group training, we evaluated the performance (in terms of success rate and execution time) of the sensorimotor-augmentation group with the XVA over three consecutive sessions in the same three reaching tasks. When comparing the success rates of sensorimotor-augmentation and motor-augmentation groups in the UR task, we did not find evidence of an interaction between group and session [$\chi^2(2) = 4.97$, $P = 0.083$, BF = 0.655]. Despite achievement of lower success rates by the sensorimotor-augmentation group, our analysis indicates no significant difference between the two groups in the second session ($P = 0.757$, BF = 0.211) or the third session ($P = 0.350$, BF = 0.263). Although the first session showcased the most substantial difference in success rate between the two groups, we did not find sufficient evidence ($P = 0.055$, BF = 1.02) to conclude that there was a distinction between them in this session either (Fig. 6A).

Integration of artificial haptic feedback did not improve coordinated XVA control

Upon comparison of the success rate of the sensorimotor-augmentation and motor-augmentation groups in the BR task, we identified an interaction between group and session [$\chi^2(2) = 12.80$, $P = 0.002$]. However, despite the sensorimotor-augmentation group achieving lower success rates, our analysis indicated no significant difference between the two groups in the second session ($P = 0.691$, BF = 0.234) or the third session ($P = 0.933$, BF = 0.239). Similarly to what was found for the UR task, even in the first session, where the most substantial difference in success rate between the groups was observed, we did not find sufficient evidence ($P = 0.095$, BF = 0.952) to conclude that there was a distinction between them (Fig. 6B).

Integration of artificial haptic feedback did not improve coordinated blindfolded XVA control

When analyzing the success rate of the sensorimotor-augmentation and motor-augmentation groups in the UR task, we found no substantial evidence indicating an interaction between group and session [$\chi^2(1) = 0.15$, $P = 0.701$, BF = 0.227]. As shown in Fig. 6C and contrary to what we would have expected, the two groups attained

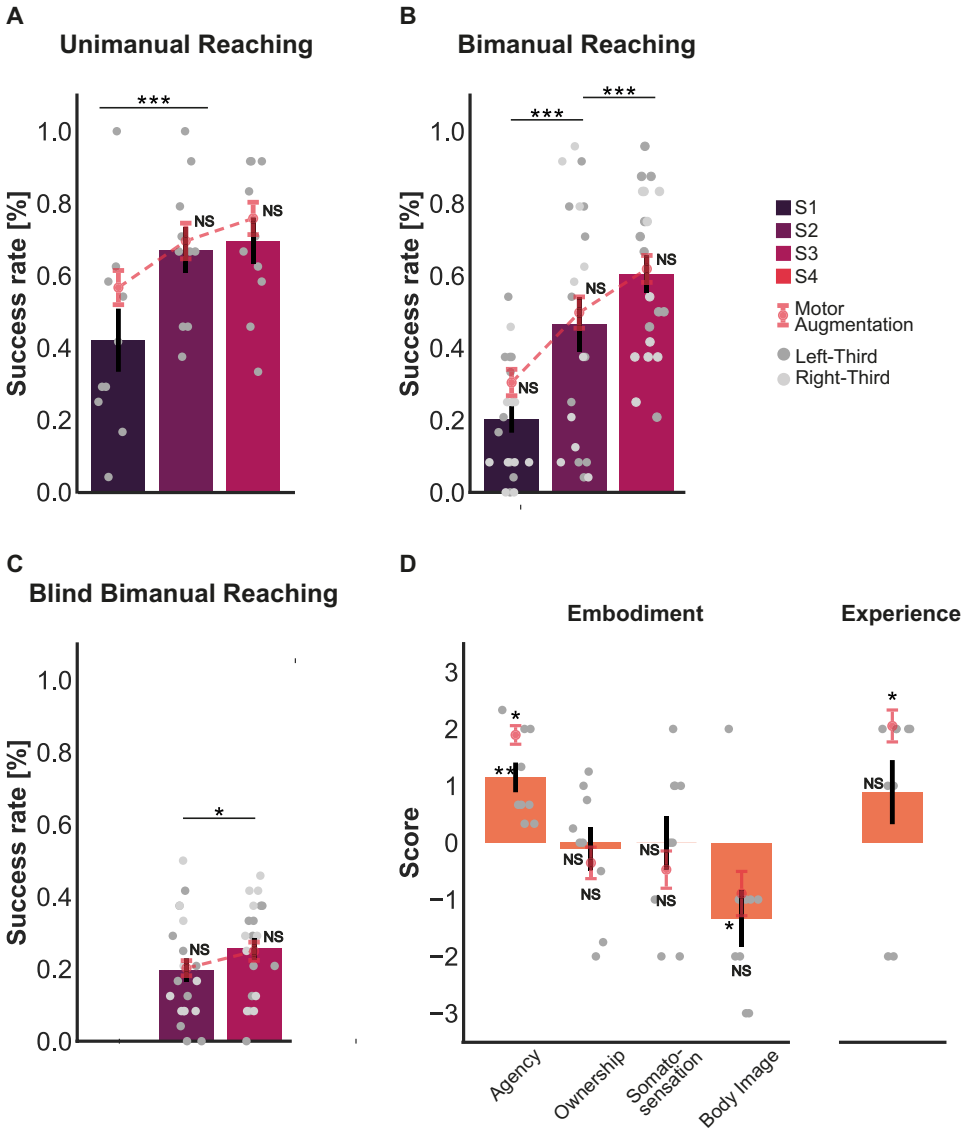

Fig. 6. Independent and coordinated sensorimotor XVA control. Average success rates for the (**A**) UR task, (**B**) BR task, and (**C**) B-BR task performed with the XVA by the sensorimotor-augmentation group in the three training sessions. Error bars represent the SEM. Each point represents a participant. Average success rate and its SE for the corresponding task performed with the XVA by the motor-augmentation group in the three training sessions are also reported for comparison. (**D**) Results of the questionnaire aiming to evaluate the embodiment and the experience with the XVA for the sensorimotor-augmentation group. The average scores are plotted for the different questions of the questionnaire together with the SEM. Each dot represents the score for a participant. Average embodiment questionnaire scores and their SEs for the motor-augmentation group are also reported for comparison. Asterisks indicate different levels of statistical significance: ***$P < 0.001$, **$P < 0.01$, and *$P < 0.05$. NS, nonsignificant difference (BF < 1).

similar success rates in both the second session ($P = 0.927$, BF = 0.296) and the third session ($P = 0.868$, BF = 0.161).

Integration of artificial haptic feedback did not boost embodiment

Contrary to what was expected, the incorporation of haptic feedback did not enhance embodiment ratings (Fig. 6D), which were comparable for ownership ($t_{16.69} = -0.52$, $P = 0.610$, BF = 0.409), somatosensation ($Z = -0.79$, $P = 0.444$, BF = 0.476), and body image ($t_{17.73} = 0.69$, $P = 0.498$, BF = 0.431) categories and lower when it came to the feeling of agency ($t_{14.49} = 2.42$, $P = 0.029$) when comparing the sensorimotor-augmentation and motor-augmentation groups. The reduced feeling of agency could be explained by the general tendency of the sensorimotor-augmentation group to exhibit lower success rates. The sensorimotor-augmentation group also rated the experience less positively compared with the motor-augmentation group ($Z = 2.25$, $P = 0.026$). Such a result might be explained by the additional wearable setup (the haptic display) that these participants had to wear.

The planar XRA prototype

To validate the usability of our HMI in the physical world, we developed a physical prototype of an XRA. Our XRA is a wearable robot

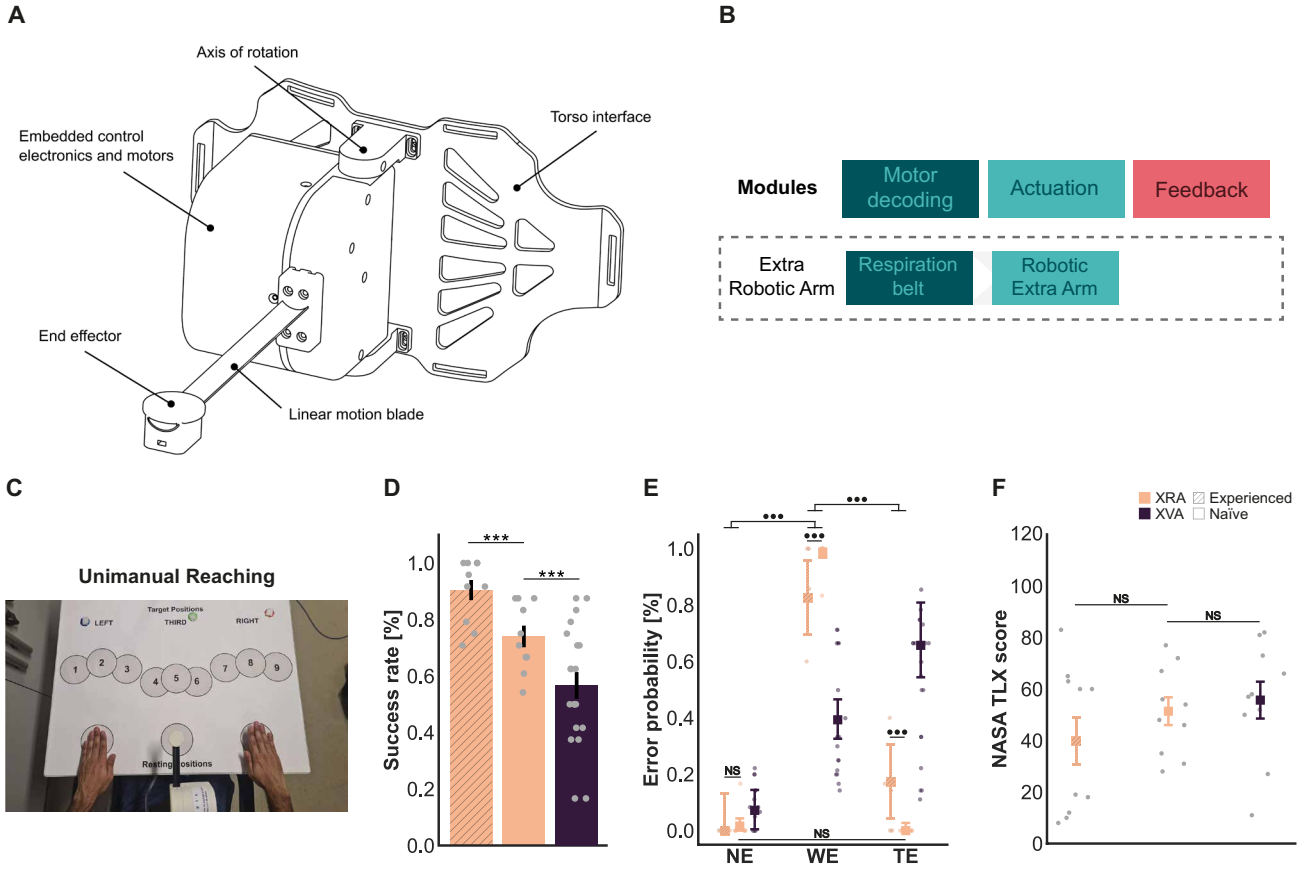

Fig. 7. XRA control assessment. (**A**) Sketch of the XRA prototype and its components. (**B**) Schematic of the motor decoding and actuation modules, following the same module principle as for the neurorobotic platform. (**C**) View of the experimental setup for the (XRA) UR task. No haptic feedback module was present for this task. The XRA was actuated via the decoding of diaphragm modulation with a respiration belt. (**D**) Average success rates for the UR task performed with the XRA by experienced and naïve participants and success rate for the UR task performed with the XVA by the motor-augmentation group in the first session. Error bars represent the SEM. Each point represents a participant. (**E**) Error probability of NE errors, WE errors, and TEs for the UR task performed with the XRA by experienced and naïve participants and success rate for the UR task performed with the XVA by the motor-augmentation group in the first session. Error bars represent the multinomial CI. Each point represents a participant, with no point reported if the participant did not commit any error. (**F**) Overall score of the NASA TLX questionnaire administered to the participants after each one of the tasks. The marker represents the mean value across participants, whereas the bar stands for its SE. Each point represents a participant. Asterisks and dots indicate different levels of statistical significance: ***$P < 0.001$, •••BF > 30. NS, nonsignificant difference (BF < 1).

weighing less than 2 kg attached to the chest of the user via adjustable straps that integrates a base allowing planar rotation and an extensible metallic band for the end-effector translation (Fig. 7A). Despite some minor oscillations in the vertical axis, the arm demonstrated smooth and consistent trajectories, showing its potential to effectively execute tasks designed on a 2D plane (fig. S8). Users could control the XRA with a simplified version of our motor HMI, where the eye-tracking module was replaced by automated orientation of the XRA toward the trial's target. The sensory HMI was not integrated for the XRA because the comparison of the evaluation block outcomes showed no improvement compared with using the motor HMI alone (Fig. 7B).

XRA control benefited from previous virtual reality training

The volunteers of the motor-augmentation group taking part in the fourth session were asked to perform a single session of UR with the XRA (Fig. 7C), serving as experienced participants given their previous experience with the HMI over the course of three consecutive days of training. We also recruited 10 additional naïve volunteers who had no previous experience with the HMI (control group, 5 females and 5 males, age = 24.6 ± 2.5), who performed this same task.

As depicted in Fig. 7D, experienced HMI users exhibited a higher success rate in the UR task with the XRA compared with naïve participants [HMI experienced: 90.4 ± 3.6%; HMI naïve: 74.0 ± 3.8%, $\chi^2(1) = 22.65$, $P < 0.001$]. Moreover, experienced users tended to show lower execution time compared with naïve users (HMI experienced: 4.3 ± 0.1 s; HMI naïve: 4.6 ± 0.1 s, $t_{12.85} = 1.93$, $P = 0.076$, BF = 1.368). See fig. S9.

Naïve users performed better with the XRA than with the XVA

We compared the UR task success rate of naïve XRA users with that of naïve XVA users (motor-augmentation group in the first session) to understand whether having the first-use experience with a virtual or physical extra arm would result in different performances (Fig. 7D). We found that a higher success rate was achieved with the XRA by naïve users [$\chi^2(1) = 21.22$, $P < 0.001$]. However, when analyzing execution times (fig. S9), in their first use, participants seemed to be faster with the

XVA (XVA naïve: 4.3 ± 0.1 s; XRA naïve: 4.6 ± 0.1%, $t_{10.54} = 2.06$, $P = 0.065$, BF = 6.317).

Incorrect execution was the primary error source in XRA-independent motor control

Analyzing the source of error when using the XRA (Fig. 7E), we found that experienced users did not commit any NE errors, whereas naïve users did not commit any TEs. Given this complete separation, we decided to base the following analysis mostly on Bayesian hypothesis testing given its stronger robustness in such cases (*42*). Although we found an interaction between group and error type [$\chi^2(12) = 8.18$, $P < 0.001$, BF = 390.76], WE error was the most frequent for both experienced and naïve users when compared with NE errors and TEs (BF > 1×10^3), with a higher frequency of occurrence in naïve users (WE experienced: 82.61, 95% CI [69.56, 95.75]%; WE naïve: 98.39, 95% CI [96.77, 1.00] %, BF = 36.75). With the frequency of occurrence of WE errors for naïve users approaching 1, NE error and TE frequencies were comparable (NE naïve: 1.61, 95% CI [0.00, 4.33]%; TE naïve: 0.00, 95% CI [0.00, 2.72]%, BF = 0.715). Given their extremely rare occurrence, NE errors and TEs can be considered negligible. Despite the large multinomial CIs, TEs were the second source of error for experienced users, with a substantial proportion compared with NE errors (NE experienced: 0.00, 95% CI [0.00, 13.14]%; TE experienced: 17.39, 95% CI [4.35, 30.53]%, BF = 7.93). Last, as expected, given our initial qualitative analysis of the data, TEs were more frequent in experienced users than in naïve volunteers (BF = 50.13), resulting in a nonnegligible proportion. In contrast, we found that the frequency of NE errors for experienced users was comparable with that for naïve users and, therefore, negligible (BF = 0.574). In summary, although both groups mainly committed WE errors, there was a separation in the secondary error types. Experienced users were more likely to commit TEs, whereas naïve users did not commit TEs at all. The frequency of NE errors was negligible for both groups.

Comparable UR task workload with the XRA and XVA at first use

After performing the UR task with the XRA, experienced and naïve participants were asked to complete the NASA TLX questionnaire to assess their perceived task workload (Fig. 7F). Despite experienced participants rating the task as less demanding, we did not find evidence of a difference between the two groups (HMI experienced: 39.8 ± 9.1%; HMI naïve: 51.4 ± 5.4%, $Z = 0.91$, $P = 0.385$, BF = 1.06). We also compared the NASA TLX scores of naïve XRA users with the scores given after the first training session with the XVA by the motor-augmentation group subgroup that completed the questionnaire to understand whether the kind of extra arm used in the first session determined differences in workload perception. Although the task was rated as more challenging when using the XVA, the scores given by the two groups were comparable ($t_{16.74} = -0.48$, $P = 0.638$, BF = 0.431).

DISCUSSION

We developed, characterized, and validated a nonintrusive HMI designed specifically for the control of XRAs by leveraging biosignals naturally involved in motor actions. Although gaze had already been proposed as a target selection mechanism triggering automated XRA reaching actions (*29*), its combination with decoding of diaphragm modulation ensured a more flexible control, allowing the user to freely and willingly control the XRA position along the selected direction of motion. Our HMI follows the principle of the neural resource allocation problem (*2*) to provide effective augmentation in healthy individuals without impairing natural limbs and biological functions.

As pointed out in a recent review (*2*), a common issue in the field of human enhancement is the lack of a systematic and quantitative assessment of performance. A unified assessment creates a common ground to evaluate the enhancement capabilities of a particular XRA HMI implementation and to compare different implementations among them. Here, we addressed this issue by proposing a multistep evaluation pipeline and developing a neurorobotic platform to extensively test HMIs for XRAs. Although the scope of the proposed pipeline is much broader than what could be thoroughly investigated in a single study, we believe that its comprehensive definition will help in framing and guiding future works in the field.

Using our approach, we were able to investigate several important questions that we believe should be answered when developing any XRAs: Can the user control the extra arm? Does the extra arm control approach impair the user's preexisting function? Can the user coordinate the extra arm with their biological upper limbs? We also advocate that these questions can be answered before the development of a specific XRA and that such testing could and should be considered to ensure an effective design of the robotic device, especially in terms of the optimal number of actively controlled degrees of freedom and sensorization for the implementation of shared control algorithms.

As shown in our study, our platform can provide useful results and guidelines for the design of the HMI. Depending on the application, some components can be simplified (for instance, the use of the exoskeleton).

Our results show that the gaze-respiration HMI is intuitive and, without the need for training, does not hinder users' ability to speak and freely gaze away from the selected target while controlling an XVA. In our test, including a single selectable target, the user was free to not only gaze away from the target but also explore the whole VE. Although, with the current implementation, this second possibility would be limited in the presence of additional selectable targets—because accidental selection of a new target changing the movement direction could happen—our result could be generalized to this broader case encompassing the presence of multiple selectable targets integrating a simple state machine (for instance, allowing target selection only when the control signal is zero). Volunteers reported no increase in mental demand when the control of the XVA was performed together with the gazing and counting task, with ratings indicating a medium mental demand. Such a result is of particular interest because it supports the intuitiveness of the proposed control approach and shows that not only do users have comparable results in terms of performance in the dual tasks but also their demand perception is not different, which suggests a lower probability of fatigue or errors arising (*43*).

We have assessed the proposed HMI for XRAs in terms of the effective augmentation provided [as formalized in (*2*)]. We claim that such a preliminary assessment of the extent to which the extra capabilities given to the user do not disrupt the intrinsic functions related to the biosignals used by HMI is a crucial step for applications in ecological settings.

We were able to show that with the proposed control strategy, participants can easily control the XVA in isolation and in

coordination with the biological limbs. Volunteers showed significant improvements in performance within only a few days of training. Motor performance also improved between sessions when controlling the XVA in coordination with the biological arms without visual feedback, even when no haptic feedback was provided.

In the isolated XVA control, we saw significant improvements in execution times over the three sessions only for the motor-augmentation group. We hypothesize that the increased cognitive load introduced by the haptic display might have prevented participants from optimizing performance in terms of both success rates and execution times. Without an explicit indication (other than the trial time-out) of completing trials as fast as possible, successful completion was prioritized at the expense of speed. When controlling the XVA in coordination with the biological limbs, participants from both groups showed no significant or meaningful differences across sessions. Similarly to what we hypothesized above, such a result might be ascribed to the higher task complexity.

Examining the retention of learning 1 week after training for the motor-augmentation group in the UR, BR, and B-BR tasks revealed promising results. Consistent performance was noted in the UR task, indicating effective skill retention. In the BR task, not only was skill retention observed but an additional performance improvement was seen, suggesting a possible "consolidation" effect in motor learning. Despite the complexity of the B-BR task, participants successfully retained the acquired skill, reinforcing the efficacy of our training protocol. Overall, these results from the fourth visit signify the successful long-term effect and efficacy of our motor augmentation approach in enduring motor learning.

Task demand assessment in a subset of the motor-augmentation group revealed a noteworthy decrease in mental demand with practice in both independent and coordinated XVA motor control. This aligns with the principle of "automaticity" in motor learning, where tasks become less cognitively loaded and more automatic with repeated practice (*44*, *45*), suggesting an improved and more efficient interaction with the XVA over time.

For both isolated and coordinated XVA controls, we found that the primary source of error was the time constraints we imposed on the tasks. This suggests that users' performance could increase when time constraints are less of interest.

At the end of the three sessions of training, participants from both groups reported sense of agency, but not ownership, over the XVA. Although such a result is coherent with previous findings on the effect of visuorespiratory synchronization on the embodiment of virtual bodies (*37*), we would have expected an increased sense of ownership over the XVA when haptic feedback on its state was provided through the haptic feedback display (*40*, *46*–*49*).

Moreover, in stark contrast with previous findings in extra robotic fingers (*5*) but especially with the wide body of evidence showing the critical role of sensory feedback in prosthetics (*39*, *50*, *51*), in our explorative assessment, we found that including haptic feedback did not boost performance. Despite examples of XRAs integrating a haptic feedback display (*13*, *16*), there are limited reports of systematic comparison between HMI for XRAs integrating a sensory feedback system or not, leaving the question of whether other encoding modalities could have better promoted sensory-motor integration.

In our study, despite the seemingly initial lower performance, that the sensorimotor-augmentation group obtained comparable performance compared with the motor-augmentation group suggests that the information provided is integrated and does not distract or confuse participants, without, however, providing additional information compared with the visual input in the UR and BR tasks. That delivering haptic feedback did not boost performance compared with visual feedback alone could be ascribed to the relatively low task complexity (*52*) and to the primary importance of vision in reaching tasks. This last remark could also explain why the provided haptic information did not improve performance in the B-BR. With participants being used to relying on vision in the UR and BR tasks, only two sessions might not be enough to learn to exploit the haptic information when decoupled from the visual one. Because we do report an improvement between the first and second execution of the B-BR, we argue that participants might attain higher performance with additional training when provided with the haptic feedback. Relatedly, although we saw a plateau in performance for the UR task, it is still to be verified whether performance in BR tasks could improve with additional training sessions and whether the haptic feedback would make a difference in later stages of learning.

More broadly, on the basis of our exploratory assessment, we cannot conclude whether with longer training, different haptic display placement, or different sensory modalities, successful sensorimotor integration of extra arms can be achieved. To fully address this question, a more extensive assessment of sensory feedback approaches exploiting the sensory complementary space [that is, the ensemble of sensory information that can be delivered without interfering with the biological limbs' sensory flow (*2*)], akin to what was done here for the motor aspect of the neural resource allocation problem, should be carried out.

Last, as a proof of concept, we evaluated a subset of experienced participants in the UR task with the XRA to prove the validity of our pipeline and the suitability of our platform to design HMIs for the control of XRAs. To understand the effect of training with the XVA on performances with the XRA, we also had naïve participants perform the UR task with the XRA. Although the XRA control was based on a simplified version of the HMI in which gaze-based target selection was replaced by automated target selection for practical reasons, the results obtained can be generalized to the complete HMI version on the basis of the largely documented human motor control findings reporting how fixation of target anticipates reaching movements (*26*, *53*–*55*). Our analysis strongly suggests that the proposed HMI can be effectively used for the independent control of an XRA prototype. Crucially, the superior performance of experienced users, with a success rate of almost 90% (22.2% higher than that of naïve users), provides compelling evidence of the efficacy of our virtual reality–based testing and training approach. This supports the notion that the skills developed and honed within the VE can be successfully translated to an XRA. We believe that training might also prove useful when testing more complex reaching tasks, such as those involving collaboration among the biological arms and the XRA, but also richer actions involving reaching, grasping, and manipulation. Although not exploited in this work, the XVA finger joints can be independently controlled, and the flexibility given by the proposed modular platform allows fast and effective design of more advanced and ecological tasks. Although the proposed HMI would not allow for the control of additional degrees of freedom as is, other strategies exploiting these and/or other biosignals—and potentially including shared control algorithms (*56*)—could be tested in such scenarios. Moreover, as previously mentioned, the appearance, kinematic chain, and anchor point of the XVA can be easily modified. Therefore, our modular platform could also allow extensive testing focused on determining the most efficient XRA design given a selected HMI.

Furthermore, the data indicate that, in their first use of the HMI, users performed 30.5% more effectively with the XRA than with the XVA. This finding is in line with previous results comparing control of simulated and extra robotic limbs (*19*) and can be explained by the inherent difference between the XVA and the XRA—its wearability—ensuring intrinsic feedback at the physical interface between the robot and the user (*2*, *57*, *58*).

Although we observed a different trend in the most prominent source of error when using the XRA compared with the XVA, we believe that the more frequent occurrence of WE errors with the XRA could be due to the setup itself and a less-accurate ability to track participants' hands' relative positions on the target board with the camera system. Together, the above observations underline the viability of our virtual reality–based testing and training protocols and the proposed pipeline.

To conclude, although the idea of human augmentation using XRAs is becoming more and more popular and widely investigated, the development of HMIs that do not rely on neural resources normally involved in daily activities and their validation for the control of extra limbs is often disregarded. For example, most of the HMIs for XRA control exploit the use of lower limb movements (*12*–*14*, *16*, *17*), limiting their usability in general activities of daily living. At the same time, the few examples of implementations with HMIs not involving control via the lower limbs (*19*–*21*) lack a comprehensive assessment in terms of influence on preexisting abilities and functionality. Last, although a handful of groundbreaking studies have initiated more systematic exploration of HMIs, those focused on 2D or 3D cursor control (*22*–*25*), despite providing valuable insights, do not encapsulate the full complexity of managing an extra limb within a 3D environment. Our current work is a step toward it by proposing a pipeline for designing and testing HMIs for XRAs. XRAs can represent the next frontier of robotics and neural engineering with important clinical and industrial impacts. However, to move these devices to applications in ecological settings, we should fully acknowledge the fundamental difference with respect to other robotics paradigms for restoration and human-robot collaboration (*2*) and develop tailored HMIs to ensure effective augmentation and embodiment of XRAs.

Here, we designed an HMI conceived for the control of XRAs and not affecting preexisting biological function. We also propose a systematic pipeline used to validate the proposed HMI that, if adopted by the community, we anticipate could play a critical role in the design of XRAs and HMIs for human augmentation.

MATERIALS AND METHODS

Participants

A total of 65 healthy able-bodied people participated in the tests and experiments described in this work (32 females and 33 males, age = 24.4 ± 3.4, all right-handed). Ten people (five females and five males, age = 25.7 ± 2.0) were recruited to assess the level of augmentation with respect to the involved biological functions attainable with the proposed HMI. Thirty able-bodied volunteers (15 females and 15 males, age = 22.95 ± 3.58) were recruited for testing and training and assigned to the motor-augmentation group (n = 20, 10 females and 10 males, age = 24.6 ± 4.4) or to the sensorimotor-augmentation group (n = 10, 5 females and 5 males, age = 22.2 ± 2.6). Ten volunteers in the motor-augmentation group (five females and five males, age = 25.4 ± 4.4) were invited for a fourth session 1 week after completion of training, whereas five volunteers (three females and two males, age = 22.8 ± 2.8) were invited for a fourth session 1 year after training. Ten healthy volunteers were recruited and assigned to the control group (five females and five males, age = 24.6 ± 2.5). Eighteen people took part in the characterization tests (see the Supplementary Materials). Some of them took part in multiple tests or were further recruited to one of the groups described above provided that they were fully naïve to the given setup. A list of all experiments and characterization tests with the corresponding number of participants involved is reported in table S1. The study was approved by the Commission Cantonale d'éthique de la recherche Genève (BASEC-ID: 2019–02176). All participants gave written informed consent to participate in the study. Each participant's visit (session) lasted between 30 and 90 min, including preparation.

Gaze-diaphragmatic respiration HMI

Visuomotor coordination is known to be involved in reaching movements, with saccades (rapid eye movement to focus the area of interest within the fovea) preceding the movement onset. Eye gaze can be therefore considered a valuable source of information when it comes to reaching intended targets, which was used previously with XRAs (*29*) and was exploited in a hybrid brain-computer interface (BCI) for the control of an upper limb exoskeleton (*28*). Here, we tracked eye movements to determine whether the user was focusing on a reachable target to reduce the control for an extra arm 3D reaching action to the control over the single degree of freedom given by the direction between the end effector and the selected target. In our proposed HMI, the user controls the movement of the extra limb by modulating the diaphragm expansion (Fig. 2C). We implemented an adaptive two-level threshold to identify the three possible stages needed to control the extra arm. To move the end effector forward, the user needed to breathe in to expand the diaphragm, whereas contraction of the diaphragm was interpreted as intention to move backward. Last, a relaxed diaphragm, with which users could breathe normally, maintained the current position. The upper limit threshold was defined as 50% of the maximum expansion over the average contraction; meanwhile, the lower limit was 50% of the minimum contraction under the average. Thresholds were updated every 100 ms. The diaphragmatic modulation signal was recorded with the respiration belt from BrainVision, connected to the ANT Neuro recording system, sampled at 512 Hz, and filtered with a high-pass Butterworth filter of second order with a cutoff frequency of 25.6 Hz.

Haptic feedback display

We developed a haptic display to provide tactile and proprioceptive feedback from an extra limb to the user. The haptic display included two modules: a tactor consisting of a 3D-printed lever system connected to a servomotor (DES 448 BB MG 10 mm, Graupner) and two coin vibration motors (Precision Microdrives Ltd., UK) (Fig. 2A). We selected a hybrid feedback-encoding strategy for contact and proprioceptive information, inspired by successful implementations with vibrators and pressure actuators in upper limb prosthetics (*59*, *60*) and its ability to prevent user discomfort by avoiding continuous vibrations (*5*). The first module, positioned on the left pectoralis, delivered pressure stimuli on the user's skin to encode the distance of an extra limb end effector from the resting position, thus providing proprioceptive information. With the extra limb hand at rest close to the body, the lever head was in contact with the skin with no indentation; when the hand moved

further away from the body, pressure was increased as a function of the distance from the resting position. The two coin vibration motors of the second module were placed on the user's chest, one on the left and one on the right side, and encoded tactile information. In particular, the left and right motors encoded making (high-intensity vibration) and breaking (low-intensity vibration) contact, respectively, with a target and with a biological arm. Each vibration lasted 250 ms per event. The two modules were controlled with an Arduino ATMega2560 via a custom MATLAB (MathWorks, USA) script, which mapped the normalized distance (with respect to the extra limb range of motion) between the minimum and maximum servomotor rotation angles of 10° and 80° and wrote it to the motor pin and controlled the coin motors' frequency intensities via pulse-width modulation.

The XVA and the modular neurorobotic platform

With the aim of testing the proposed HMI in a flexible setting, we developed an immersive VE where a humanoid avatar controlled by the user is endowed with an extra upper limb—the XVA. To avoid association with a left or right limb, the hand of the XVA has four fingers and two thumbs (Fig. 2A). In the experiments described here, to maintain symmetry of the body, the XVA was always positioned in the middle of the chest; however, the XVA anchor point can be chosen at will. The XVA is characterized by a custom-configured kinematic chain inspired by the human arm (see the Supplementary Materials) and, thus, is controlled using inverse kinematics, giving as input the position and orientation of the end effector (the XVA hand). The VE, with the avatar in first-person perspective, was developed in Unity (Unity Technologies, USA) and was rendered to participants wearing the Vive Pro Eye HMD (HTC Corporation, Taiwan). The VE and its components are the core of the proposed modular testing platform, which accounts for a control loop and a sensory loop, with different implementations for the XVA and the natural arms (Fig. 2B).

For the motor control of the XVA using our proposed gaze-diaphragmatic respiration HMI, we capitalized on the Tobii eye tracking system embedded in the Vive Pro Eye HMD and on the TobiiXR eye tracking SDK. The platform then accepted a three-class classification result reflecting the user intention to move forward or backward or to stay still. In our implementation, this is the output of our diaphragmatic modulation decoding; however, the level of abstraction given by the platform potentially allows any other classification output to complement gaze in such an HMI. At present, the rotation of the third hand is automated in such a way that while approaching the target for BR, the wrist supinates to face the target with the palm of the third hand.

ALEx [(*41*, *61*); Wearable Robotics Srl, Italy] allowed the control of the avatar's "natural" arms. ALEx's left and right arm exoskeletons are characterized by six rotational degrees of freedom serially connected to constitute a kinematic chain ensuring kinematic isomorphism with the human arm. The three shoulder and one elbow degrees of freedom are actuated. The mobility ranges of the six degrees of freedom cover about 92% of the human arm's workspace. A proprietary Wearable Robotics application allowed bidirectional communication between the ALEx station and the platform, which translated the user's shoulder and elbow joint orientations tracked by ALEx into the virtual natural arm joints in real time. To ensure accurate tracking, utmost care was taken when adjusting the position of the exoskeleton to fit the user, and tracking was qualitatively assessed in the VE before starting the experiments (making sure that clasped biological hands resulted in clasped left and right hands of the avatar).

The Unity physics engines allowed the simulation of realistic behaviors in the VE, providing useful information that, together with the detailed knowledge of the environmental objects' relative positions, we exploited to deliver haptic feedback to the user. In particular, we used the proposed haptic feedback display to provide the user with information about the XVA contact—either with a target or one of the biological arms—and about the proximity of the XVA to the target. For this, the relevant information from the VE was streamed to display delivering mechanical stimulations on the user's chest skin.

When it comes to the biological arms, although proprioception is inherently ensured by the adopted tracking approach, we also exploited the possibility of applying torques to the ALEx's joints to provide force feedback based on collisions in the VE. We used Lab Streaming Layer for real-time networking of the different modules and collection of relevant data.

The planar XRA

We developed a prototype of an XRA to test our HMI with a physical robot. Our XRA is a wearable robot attached to the chest of the user via adjustable straps and integrates a base allowing planar rotation and a linear motion blade for the end-effector translation (Fig. 7A). The overall weight of the robot is less than 2 kg, and its weight distribution is located close to the chest, which makes it comfortable to use. The weight distribution is also only marginally affected by the extension of the metal band because it is very lightweight. The workspace spans over 36° in rotation and 40 cm in translation with a speed of 8.5 cm/s at a precision of 0.4 cm/s. The XRA controller runs on an Arduino Due and receives input for rotation and translation via serial communication. At present, the target selection, which determines the XRA orientation, is automated and not based on eye tracking as in the case of the XVA HMI implementation. The end-effector translation is based on the diaphragmatic respiration modulation decoder classification output in the same way as for the XVA HMI.

The movement trajectories of the XRA were characterized to assess the robot's movement stability and smoothness (fig. S8). In particular, fig. S8C shows the trajectory of the XRA when moving forward toward the three possible targets for the three coordinates separately. Although the movement on the x-y plane proved to be smooth and consistent, more evident oscillations were present on the z (vertical) axis. However, we do not believe that these oscillations hindered our results because the reaching task to be performed was constrained to the 2D plane.

HMI augmentation assessment

To evaluate the level of actual augmentation provided to the user, we designed two dual tasks to investigate to what extent the gaze-diaphragm HMI interferes with the ability of the user to perform daily activities. In particular, we separately tested the effect on gaze and speech production of a UR task in virtual reality. A UR trial was considered successful if the participant reached the target and stopped inside it for 500 ms, with a trial time-out set to 5 s. To evaluate the influence on the ability to visually explore the surroundings, we had participants perform the UR task with the XVA alone while also popping a soap bubble (UR-V task) appearing in the peripheral field of view. To be popped, a bubble needed to be stared at for at least 500 ms.

Of the 24 trials, only 20 contained a bubble. A trial was considered successful only if the participant performed well on both the UR task and the popping of the bubble. On the other hand, to evaluate the effect of the diaphragm-based HMI on the ability to speak, we asked participants to count forward from 100 while controlling the XVA to perform the UR task (UR-C task). Participants could count in their preferred language so as to not add additional mental effort. A trial was successful only if the participant could perform the reaching task and if the time of motor control of the XVA while counting forward without errors was at least 40% of the time of motor control (see the Supplementary Materials and fig. S10). Participants were given detailed information on each task and the requirements for a successful execution before starting. Examples of these tasks can be found in movie S1.

UR and BR tasks

To assess the chosen sensorimotor control approach in the context of human augmentation, we defined two reaching tasks that participants performed in the VE: a UR task performed with each of the three arms (24 movements per arm) and aimed at assessing the level of independence and a BR task performed with each of the three pairs of arms (24 movements per pair) and aimed at assessing coordination. In the UR task, a trial was considered successful if the participant reached the target (a sphere with a 5-cm radius appearing in three possible locations 13 cm in front of the arm involved in the current trial) and stopped inside it for 500 ms. Trial time-out was set to 5 s. In the BR task, a trial was considered successful if the participant collided the two hands inside the target (a sphere with a 5-cm radius appearing in three possible locations 23 cm in front of the two arms involved in the current trial) within 500 ms from the moment in which the first hand entered the target. Trial time-out was set to 10 s. For both tasks, the participants had to maintain the arm(s) not involved in the reaching movement in the rest position (identified by a sphere for each arm where the hand can rest if the arm is not extended and the angle between the arm and the forearm is approximately 90°). Participants were involved in three sessions over three consecutive days, where they performed the UR and BR tasks. During the second and third sessions, the participants also performed the BR task without visual feedback from the three arms (B-BR). The choice of focusing on the coordination task to implement a blindfolded version aimed to challenge skills with the most complex task while mitigating fatigue-based confounds that could have arisen upon also introducing a blind version of the UR task. A subset of participants from the motor-augmentation group came back for a fourth session 1 week after completing the training. In this session, they performed the UR, BR, and B-BR tasks again. All study participants controlled the XVA using the gaze-diaphragm HMI. Participants in the sensorimotor-augmented group were also asked to wear the haptic display and received artificial feedback for the XVA. All participants were given detailed information on each task and the requirements for a successful execution before starting. Examples of these tasks can be found in movie S2.

XRA control assessment

In the fourth session, the subset of participants from the motor-augmentation group also performed an analogous UR task with the XRA. For the UR with the XRA, all the possible targets were numbered and displayed as circles (radius, 5 cm) on a table in front of the participants (see fig. S3A), and for each trial (24 per arm), a screen informed them of the arm and the target number to reach. The three targets for both the right and left arm were positioned at around 25 cm from the corresponding resting positions (fig. S8A). To ensure optimal visibility in the physical task (where targets and resting positions lay on the same plane), we took advantage of the extended translational capabilities of the XRA and positioned its targets at 20 cm with respect to the XRA's resting position. To match the UR task with the XRA and the XVA, the linear velocity of the XRA was set equal to the one of the XVA, around 8.5 cm/s. Therefore, because of the longer distance to be covered by the XRA, the trial time-out was adjusted and fixed to 7.6 s. The participants were asked to maintain the arms not involved in the reaching movement in the rest positions (three circles of 5-cm radius). To track the position of the XRA end effector and that of the left and right hand, we implemented a tracking system using an Intel RealSense D435 Depth Camera (Intel) and developed a MATLAB application. Three markers colored red, blue, and green (RGB) were used and located using an RGB filter. The depth information given by the camera was used to correct for the wrong optical projection due to the movement on the vertical axis. Naïve participants (control group) undertook a single session of the UR task with the XRA. All participants were given detailed information about the task and the requirements for a successful execution before starting. Video examples of these tasks can be found in movie S3.

Assessment of simultaneous speech and XVA control

The percentage of simultaneous control in terms of movement of the XVA and speaking activity was computed for the UR-C task to ensure that participants were not segregating the two aspects of the task. To do so, the control signals were rectified and interpolated to have the same sampling frequency as the speech recordings. The duration of motor control was defined as the amount of time the XVA was moving plus the last 500 ms where the participant managed to stop inside the target. Speech recordings were rectified, smoothed with a moving average over 10 ms, and made discrete with values of 0 or 1 by thresholding the audio signals. The control and speech signals were then multiplied to find the amount of simultaneous activity. To consider a trial successful, we required a minimal amount of simultaneous activity corresponding to a threshold of 40% (see the Supplementary Materials and fig. S10).

Motor performance outcome measures

We evaluated the reaching performances of participants in terms of success rate (number of correct trials divided by total number of trials) for each task and session. For BR tasks, we pooled together the trials involving the XVA and the left arm together with those involving the XVA and the right arm.

To understand the source of errors in the different tasks, we analyzed the unsuccessful trials and clustered the errors according to three categories: NE, WE, and TE. We considered NE trials to be those in which the XVA or XRA did not exit the rest position, TE trials to be those in which the participant failed because they did not meet the required timing constraints, and WE trials to be those failed because of all the remaining errors. WE errors could have different natures in the UR and BR (or B-BR) tasks. In the UR task, they included the cases in which the extra arm did not stop at all or did not stop inside the target; cases in which the reaching movement execution was correct with the extra arm, but one or both of the biological arms were not kept in the rest position; and combinations of these

Table 1. Embodiment questionnaire. Embodiment questions categorized into four distinct groups representing different aspects of embodiment.

Body ownership
1. It felt like I had three arms.
2. It seemed like the third arm was a foreign body (negative).
3. It seemed like the third arm belonged to me.
4. It seemed like the third arm was part of my body.
Agency
1. It seemed like I was in control of the third arm.
2. It seemed like I was causing the movement of the third arm.
3. It seemed like the third arm was moving on its own (negative).
Body image
1. It seemed like I was looking directly at my own arm rather than a virtual third arm.
Somatosensation
1. I could feel the position of the third arm.
Control questions
1. It felt as if I had two bodies.
2. It felt as if I had two right arms.
3. It felt as if I had two left arms.
Experience
1. I found the experience enjoyable.

cases. In the BR and B-BR tasks, in contrast, they included cases in which the collision of the two hands involved in the task happened with one or both the hands outside of the target; cases in which the BR movement execution was correct, but the biological arm not involved in the movement did not maintain the rest position; and combinations of these cases.

In UR-V and UR-C tasks, only the trials considered overall correct—that is, those trials where both tasks were accomplished—were used for the computation of success rates. Trials containing counting errors in the UR-C task were also considered unsuccessful. On the other hand, for the characterization of error sources, we considered the trials where the reaching was unsuccessful, regardless of whether the secondary task was accomplished. Last, motor performance was also assessed by computing the execution time in successful trials. Again, for BR tasks, we made no distinction between the trials involving the XVA and the right arm and those involving the XVA and the left arm.

NASA TLX questionnaires

After the UR tasks performed with the XVA during the HMI augmentation assessment, participants were asked to complete the NASA TLX questionnaire (*62*), which aims to evaluate the level of workload perceived by the participant during the task. The questionnaire consists of six questions investigating the perception of mental, physical, and temporal demand; the perception of the participants' own performance; the level of effort required; and the level of frustration perceived. The combined score of these questions provides an overall index of mental workload, with higher values corresponding to higher perceived workload. The same questionnaire was administered after each task during the three training sessions and the fourth session for the subset of motor-augmentation participants who were invited for the fourth visit. Each participant performing the UR task with the XRA also filled out the NASA TLX questionnaire at the end of the task.

Embodiment and experience questionnaires

We asked participants to complete a questionnaire at the end of their three sessions of training (Table 1) to evaluate embodiment of the XVA and their experience with it. Volunteers were asked to rate their agreement from strongly disagree to strongly agree on a seven-point Likert scale (−3, strongly disagree; 3, strongly agree) for 14 statements, based on (*7*), which aimed to investigate four aspects of embodiment (body ownership, agency, somatosensation, and body image), the participant's experience, and the volunteer's reliability in answering these kinds of questionnaires (via questions posing unrealistic scenarios). Because of data collection issues, one sensorimotor-augmentation participant did not complete the questionnaire. We averaged the scores within each of the six categories (considering the opposite value for the statement on the foreign body in the body ownership category and for the one on autonomous movement of the XVA in the agency category), and we excluded one motor-augmentation participant from the analysis because their average score in the control category exceeded 0 (neutral).

Diaphragm modulation analysis

To understand the strategy used by participants when controlling the XVA with the proposed HMI, we analyzed diaphragmatic respiration in successful trials for the UR, BR, and B-BR tasks. For each participant, session, and task—after detrending and interpolating the data to obtain sequences of the same length (corresponding to the average length of the diaphragmatic profiles)—we averaged the diaphragmatic profiles using trainable time warping (TTW) to align the different time series (*63*). To understand whether an underlying common structure exists for diaphragmatic profiles in different tasks, we clustered the time series using the TTW distance as distance measure.

Statistical analysis

Statistical analyses were performed using R (version 4.1.1). Normality was tested on nonbinomial data using the Shapiro-Wilk test. All datasets characterized by a repeated measure design were analyzed with generalized linear mixed models (GLMMs). With the exception of binomial data, for which the logit link can be directly specified when fitting the GLMM, data not normally distributed (BR execution times and NASA TLX scores) were log-transformed, and a Gaussian GLMM (therefore a linear mixed model) was used to analyze the data. For all other analyses, we used logistic regressions for binomial data, whereas one- or two-sample t tests were used when data were normally distributed, and one- or two-sample Wilcoxon signed-rank tests were used for nonbinomial and nonnormally distributed data. We used a significance level of $\alpha = 0.05$ to determine statistical significance, and Tukey adjustment was used for multiple comparisons. We extended our analysis of nonsignificant results by conducting Bayesian tests with a continuous prior distribution, specifically using a Cauchy prior width of $r = 0.707$.

Supplementary Materials

This PDF file includes:
Methods
Figs. S1 to S13
Table S1

Other Supplementary Material for this manuscript includes the following:
Movies S1 to S3
MDAR Reproducibility Checklist

REFERENCES AND NOTES

1. S. L. Washburn, Tools and human evolution. *Sci. Am.* **203**, 62–75 (1960).
2. G. Dominijanni, S. Shokur, G. Salvietti, S. Buehler, E. Palmerini, S. Rossi, F. De Vignemont, A. d'Avella, T. R. Makin, D. Prattichizzo, S. Micera, The neural resource allocation problem when enhancing human bodies with extra robotic limbs. *Nat. Mach. Intell.* **3**, 850–860 (2021).
3. D. Prattichizzo, M. Pozzi, T. Lisini Baldi, M. Malvezzi, I. Hussain, S. Rossi, G. Salvietti, Human augmentation by wearable supernumerary robotic limbs: Review and perspectives. *Prog. Biomed. Eng.* **3**, 042005 (2021).
4. J. Eden, M. Bräcklein, J. Ibáñez, D. Y. Barsakcioglu, G. Di Pino, D. Farina, E. Burdet, C. Mehring, Principles of human movement augmentation and the challenges in making it a reality. *Nat. Commun.* **13**, 1345 (2022).
5. I. Hussain, L. Meli, C. Pacchierotti, G. Salvietti, D. Prattichizzo, Vibrotactile haptic feedback for intuitive control of robotic extra fingers, in *2015 IEEE World Haptics Conference (WHC)* (IEEE, 2015), pp. 394–399.
6. T. Lisini Baldi, N. D'Aurizio, C. Gaudeni, S. Gurgone, D. Borzelli, A. D'Avella, D. Prattichizzo, Exploiting intrinsic kinematic null space for supernumerary robotic limbs control, in *2023 IEEE International Conference on Robotics and Automation (ICRA)* (IEEE, 2023), pp. 11957–11963.
7. P. Kieliba, D. Clode, R. O. Maimon-Mor, T. R. Makin, Robotic hand augmentation drives changes in neural body representation. *Sci. Robot.* **6**, eabd7935 (2021).
8. A. Shafti, S. Haar, R. Mio, P. Guilleminot, A. A. Faisal, Playing the piano with a robotic third thumb: Assessing constraints of human augmentation. *Sci. Rep.* **11**, 21375 (2021).
9. I. Hussain, G. Salvietti, G. Spagnoletti, D. Prattichizzo, The soft-sixthfinger: A wearable EMG controlled robotic extra-finger for grasp compensation in chronic stroke patients. *IEEE Robot. Autom. Lett.* **1**, 1000–1006 (2016).
10. G. Salvietti, I. Hussain, D. Cioncoloni, S. Taddei, S. Rossi, D. Prattichizzo, Compensating hand function in chronic stroke patients through the robotic sixth finger. *IEEE Trans. Neural Syst. Rehabil. Eng.* **25**, 142–150 (2017).
11. T. Aoyama, H. Shikida, R. Schatz, Y. Hasegawa, Operational learning with sensory feedback for controlling a robotic thumb using the posterior auricular muscle. *Adv. Robot.* **33**, 243–253 (2019).
12. E. Abdi, E. Burdet, M. Bouri, H. Bleuler, Control of a supernumerary robotic hand by foot: An experimental study in virtual reality. *PLOS ONE* **10**, e0134501 (2015).
13. M. Y. Saraiji, T. Sasaki, K. Minamizawa, M. Inami, MetaArms: Body remapping using feet-controlled artificial arms, in *Proceedings of the 31st Annual ACM Symposium on User Interface Software and Technology,* (ACM, 2018), pp. 140–142.
14. W. Amanhoud, J. Hernandez Sanchez, M. Bouri, A. Billard, Contact-initiated shared control strategies for four-arm supernumerary manipulation with foot interfaces. *Int. J. Robot. Res.* **40**, 986–1014 (2021).
15. A. Noccaro, J. Eden, G. Di Pino, D. Formica, E. Burdet, Human performance in three-hands tasks. *Sci. Rep.* **11**, 9511 (2021).
16. K. Arai, H. Saito, M. Fukuoka, S. Ueda, M. Sugimoto, M. Kitazaki, M. Inami, Embodiment of supernumerary robotic limbs in virtual reality. *Sci. Rep.* **12**, 9769 (2022).
17. Y. Huang, J. Eden, E. Ivanova, E. Burdet, Human performance of three hands in unimanual, bimanual and trimanual tasks. *Annu Int. Conf. IEEE Eng. Med. Biol. Soc. EMBC*, 1493–1497 (2022).
18. J. Hernandez Sanchez, W. Amanhoud, A. Billard, M. Bouri, Enabling four-arm laparoscopic surgery by controlling two robotic assistants via haptic foot interfaces. *Int. J. Robot. Res.* **42**, 475–503 (2023).
19. F. Parietti, H. H. Asada, Independent, voluntary control of extra robotic limbs, in *2017 IEEE International Conference on Robotics and Automation* (IEEE, 2017), pp. 5954–5961.
20. C. I. Penaloza, S. Nishio, BMI control of a third arm for multitasking. *Sci. Robot.* **3**, eaat1228 (2018).
21. J. Guggenheim, R. Hoffman, H. Song, H. H. Asada, Leveraging the human operator in the design and control of supernumerary robotic limbs. *IEEE Robot. Autom. Lett.* **5**, 2177–2184 (2020).
22. L. Bashford, J. Wu, D. Sarma, K. Collins, R. P. N. Rao, J. G. Ojemann, C. Mehring, Concurrent control of a brain–computer interface and natural overt movements. *J. Neural Eng.* **15**, 066021 (2018).
23. S. Gurgone, D. Borzelli, P. de Pasquale, D. J. Berger, T. Lisini Baldi, N. D'Aurizio, D. Prattichizzo, A. d'Avella, Simultaneous control of natural and extra degrees of freedom by isometric force and electromyographic activity in the muscle-to-force null space. *J. Neural Eng.* **19**, 016004 (2022).
24. M. Bräcklein, J. Ibáñez, D. Barsakcioglu, D. Farina, Towards human motor augmentation by voluntary decoupling beta activity in the neural drive to muscle and force production. *J. Neural Eng.* **18**, 016001 (2021).
25. D. J. L. L. Pinheiro, J. Faber, S. Micera, S. Shokur, Human-machine interface for two-dimensional steering control with the auricular muscles. *Front. Neurorobot.* **17**, 1154427 (2023).
26. L. Lünenburger, D. F. Kutz, K.-P. Hoffmann, Influence of arm movements on saccades in humans. *Eur. J. Neurosci.* **12**, 4107–4116 (2000).
27. V. Novak, R. Riener, Predicting targets of human reaching motions with an arm rehabilitation exoskeleton. *Biomed. Sci. Instrum.* **51**, 385–392 (2015).
28. A. Frisoli, C. Loconsole, D. Leonardis, F. Banno, M. Barsotti, C. Chisari, M. Bergamasco, A new gaze-BCI-driven control of an upper limb exoskeleton for rehabilitation in real-world tasks. *IEEE Trans. Syst. Man Cybern. Part C Appl. Rev.* **42**, 1169–1179 (2012).
29. Z. Fan, C. Lin, C. Fu, A gaze signal based control method for supernumerary robotic limbs, in *2020 3rd International Conference on Control and Robots* (IEEE, 2020), pp. 107–111.
30. S. C. Gandevia, J. C. Rothwell, Activation of the human diaphragm from the motor cortex. *J. Physiol.* **384**, 109–118 (1987).
31. E. Vanegas, R. Igual, I. Plaza, Sensing systems for respiration monitoring: A technical systematic review. *Sensors* **20**, 5446 (2020).
32. L. Marchal-Crespo, R. Zimmermann, O. Lambercy, J. Edelmann, M.-C. Fluet, M. Wolf, R. Gassert, R. Riener, Motor execution detection based on autonomic nervous system responses. *Physiol. Meas.* **34**, 35 (2012).
33. R. Zimmermann, L. Marchal-Crespo, J. Edelmann, O. Lambercy, M.-C. Fluet, R. Riener, M. Wolf, R. Gassert, Detection of motor execution using a hybrid fNIRS-biosignal BCI: A feasibility study. *J. NeuroEng. Rehabil.* **10**, 4 (2013).
34. H.-D. Park, C. Barnoud, H. Trang, O. A. Kannape, K. Schaller, O. Blanke, Breathing is coupled with voluntary action and the cortical readiness potential. *Nat. Commun.* **11**, 289 (2020).
35. H.-D. Park, T. Piton, O. A. Kannape, N. W. Duncan, K.-Y. Lee, T. J. Lane, O. Blanke, Breathing is coupled with voluntary initiation of mental imagery. *Neuroimage* **264**, 119685 (2022).
36. A. Monti, G. Porciello, G. Tieri, S. M. Aglioti, The "embreathment" illusion highlights the role of breathing in corporeal awareness. *J. Neurophysiol.* **123**, 420–427 (2019).
37. D. Adler, B. Herbelin, T. Similowski, O. Blanke, Breathing and sense of self: Visuo–respiratory conflicts alter body self-consciousness. *Respir. Physiol. Neurobiol.* **203**, 68–74 (2014).
38. G. G. Wang, Definition and review of virtual prototyping. *J. Comput. Inf. Sci. Eng.* **2**, 232–236 (2003).
39. F. Clemente, M. D'Alonzo, M. Controzzi, B. B. Edin, C. Cipriani, Non-invasive, temporally discrete feedback of object contact and release improves grasp control of closed-loop myoelectric transradial prostheses. *IEEE Trans. Neural Syst. Rehabil. Eng.* **24**, 1314–1322 (2016).
40. P. Svensson, U. Wijk, A. Björkman, C. Antfolk, A review of invasive and non-invasive sensory feedback in upper limb prostheses. *Expert Rev. Med. Devices* **14**, 439–447 (2017).
41. M. Bergamasco, F. Salsedo, B. Lenzo, An exoskeleton structure for physical interaction with a human being (2013); https://patents.google.com/patent/WO2013186705A3/en.
42. J. K. Kruschke, *Doing Bayesian Data Analysis: A Tutorial with R, JAGS, and Stan* (Academic Press, ed. 2, 2014).
43. Y. Y. Yurko, M. W. Scerbo, A. S. Prabhu, C. E. Acker, D. Stefanidis, Higher mental workload is associated with poorer laparoscopic performance as measured by the NASA-TLX tool. *Simul. Healthc.* **5**, 267–271 (2010).
44. K. DeLeeuw, R. Mayer, A comparison of three measures of cognitive load: Evidence for separable measures of intrinsic, extraneous, and germane load. *J. Educ. Psychol.* **100**, 223–234 (2008).
45. S. Kobori, Y. Abe, Pupillary responses during learning of inverted tracking tasks, in *World Congress on Medical Physics and Biomedical Engineering,* IFMBE Proceedings (Springer, 2009), pp. 211–214.
46. H. H. Ehrsson, The concept of body ownership and its relation to multisensory integration. *New Handb. Multisensory Process.* **104**, 775–792 (2012).
47. H. H. Ehrsson, N. P. Holmes, R. E. Passingham, Touching a rubber hand: Feeling of body ownership is associated with activity in multisensory brain areas. *J. Neurosci.* **25**, 10564–10573 (2005).
48. P. D. Marasco, J. S. Hebert, J. W. Sensinger, D. T. Beckler, Z. C. Thumser, A. W. Shehata, H. E. Williams, K. R. Wilson, Neurorobotic fusion of prosthetic touch, kinesthesia, and movement in bionic upper limbs promotes intrinsic brain behaviors. *Sci. Robot.* **6**, eabf3368 (2021).
49. K. Umezawa, Y. Suzuki, G. Ganesh, Y. Miyawaki, Bodily ownership of an independent supernumerary limb: An exploratory study. *Sci. Rep.* **12**, 2339 (2022).
50. V. Mendez, F. Iberite, S. Shokur, S. Micera, Current solutions and future trends for robotic prosthetic hands. *Annu. Rev. Control Robot. Auton. Syst.* **4**, 595–627 (2021).

51. S. J. Bensmaia, D. J. Tyler, S. Micera, Restoration of sensory information via bionic hands. *Nat. Biomed. Eng.* **7**, 443–455 (2023).
52. R. Sigrist, G. Rauter, R. Riener, P. Wolf, Augmented visual, auditory, haptic, and multimodal feedback in motor learning: A review. *Psychon. Bull. Rev.* **20**, 21–53 (2013).
53. R. Herman, R. Herman, R. Maulucci, Visually triggered eye-arm movements in man. *Exp. Brain Res.* **42**, 392–398 (1981).
54. R. S. Johansson, G. Westling, J. Anders Bäckström, R. Flanagan, Eye–hand coordination in object manipulation. *J. Neurosci.* **21**, 6917–6932 (2001).
55. J. D. Crawford, W. P. Medendorp, J. J. Marotta, Spatial transformations for eye–hand coordination. *J. Neurophysiol.* **92**, 10–19 (2004).
56. K. Z. Zhuang, N. Sommer, V. Mendez, S. Aryan, E. Formento, E. D'Anna, F. Artoni, F. Petrini, G. Granata, G. Cannaviello, W. Raffoul, A. Billard, S. Micera, Shared human–robot proportional control of a dexterous myoelectric prosthesis. *Nat. Mach. Intell.* **1**, 400–411 (2019).
57. J. L. Pons, *Wearable Robots: Biomechatronic Exoskeletons* (John Wiley & Sons, 2008).
58. J. W. Guggenheim, H. H. Asada, Inherent haptic feedback from supernumerary robotic limbs. *IEEE Trans. Haptics* **14**, 123–131 (2021).
59. F. Clemente, C. Cipriani, A novel device for multi-modal sensory feedback in hand prosthetics: Design and preliminary prototype, in *2014 IEEE Haptics Symposium* (IEEE, 2014), pp. 569–573 (2014).
60. H. Huang, T. Li, C. Bruschini, C. Enz, J. Justiz, C. Antfolk, V. M. Koch, Multi-modal sensory feedback system for upper limb amputees, in *2017 New Generation of CAS (NGCAS)* (IEEE, 2017), pp. 193–196.
61. E. Galofaro, E. D'Antonio, N. Lotti, F. Patané, M. Casadio, L. Masia, Bimanual motor strategies and handedness role in human-robot haptic interaction. *IEEE Trans. Haptics* **16**, 296–310 (2023).
62. S. G. Hart, L. E. Staveland, Development of NASA-TLX (task load index): Results of empirical and theoretical research. *Adv. Psychol.* **52**, 139–183 (1988).
63. S. Khorram, M. G. McInnis, E. M. Provost, Trainable time warping: Aligning time-series in the continuous-time domain, in *IEEE International Conference on Acoustics, Speech and Signal Processing (ICASSP)* (IEEE, 2019), pp. 3502–3506.

Acknowledgments: We thank the Foundation Campus Biotech Geneva Virtual Reality and Robotics Facility for the support in developing the virtual environment. We thank F. Maenza for the help with data collection. We thank M. Gafsou for granting us permission to use and modify their photograph for inclusion in this paper. G.D. is the Bertarelli Foundation Chair in Translational Neural Engineering. B.O. is the Bertarelli Foundation Chair in Cognitive Neuroprosthetics. **Funding:** This project was partly funded by the Bertarelli Foundation, by the Swiss National Science Foundation via the National Competence Center Research (NCCR) Robotics, and by the "European Union's Horizon 2020 MSCA Program"' under grant agreement no. 813713, the Coordenação de Aperfeiçoamento e Pessoal de Nível Superior–Brazil (CAPES)–Financial Code 001, and the CAPES PrInt initiative. **Author contributions:** G.D., C.P., S.S., and S.M. conceived and designed the study. G.D. developed the modular platform. B.O. developed the diaphragm modulation decoder. J.O. developed the planar extra robotic arm. G.D. and E.A. developed the haptic display. G.D., D.L.P., L.P., and M.G. performed the experiments. G.D., D.L.P., and L.P. analyzed the data. G.D., L.P., S.S., and S.M. wrote the manuscript with input from every coauthor. **Competing interests:** The authors declare that they have no competing interests. **Data and materials availability:** All data needed to evaluate the conclusions in this paper are present in the paper or the Supplementary Materials. The data and codes for this study have been deposited in the database 10.5281/zenodo.10107896.

Submitted 13 February 2023
Accepted 15 November 2023
Published 13 December 2023
10.1126/scirobotics.adh1438

Science Robotics

Human motor augmentation with an extra robotic arm without functional interference

Giulia Dominijanni, Daniel Leal Pinheiro, Leonardo Pollina, Bastien Orset, Martina Gini, Eugenio Anselmino, Camilla Pierella, Jérémy Olivier, Solaiman Shokur, and Silvestro Micera

Sci. Robot. **8** (85), eadh1438. DOI: 10.1126/scirobotics.adh1438

Science Robotics (ISSN 2470-9476) is published by the American Association for the Advancement of Science. 1200 New York Avenue NW, Washington, DC 20005. The title *Science Robotics* is a registered trademark of AAAS.